Experimental Measurements of Thermoelectric Phenomena in Nanoparticle Liquid Suspensions (Nanofluids)

by

Moxuan Zhu

A Thesis Presented in Partial Fulfillment
of the Requirements for the Degree
Master of Science

Approved November 2010 by the
Graduate Supervisory Committee:

Patrick Phelan, Chair
Steven Trimble
Ravi Prasher

ARIZONA STATE UNIVERSITY

December 2010

ABSTRACT

This study analyzes the thermoelectric phenomena of nanoparticle suspensions, which are composed of liquid and solid nanoparticles that show a relatively stable Seebeck coefficient as bulk solids near room temperature. The approach is to explore the thermoelectric character of the nanoparticle suspensions, predict the outcome of the experiment and compare the experimental data with anticipated results. In the experiment, the nanoparticle suspension is contained in a 15cm*2.5cm*2.5cm glass container, the temperature gradient ranges from 20 °C to 60 °C, and room temperature fluctuates from 20 °C to 23°C. The measured nanoparticles include multiwall carbon nanotubes, aluminum dioxide and bismuth telluride. A temperature gradient from 20 °C to 60 °C is imposed along the length of the container, and the resulting voltage (if any) is measured. Both heating and cooling processes are measured. With three different nanoparticle suspensions (carbon nano tubes, Al_2O_3 nanoparticles and Bi_2Te_3 nanoparticles), the correlation between temperature gradient and voltage is correspondingly 8%, 38% and 96%. A comparison of results calculated from the bulk Seebeck coefficients with our measured results indicate that the Seebeck coefficient measured for each suspension is much more than anticipated, which indicates that the thermophoresis effect could have enhanced the voltage. Further research with a closed-loop system might be able to affirm the results of this study.

TABLE OF CONTENTS

Page

LIST OF TABLES

LIST OF FIGURES

Figure Page

CHAPTER 1 INTRODUCTION

The thermoelectric phenomena was discovered nearly two centuries ago, first by Thomas Seebeck and Jean Peltier, which is regarded as the basis of the modern thermoelectric industry (Tellurex, 2010). This phenomenon indicates that a junction made from two different kinds of materials, usually conductors, would show a flow of electrical current when a temperature gradient is applied to it. On the other hand, Peltier found that when electrical current is applied, the two different materials of the junction would either absorb or release energy (in the form of heat). Nowadays, we are able to explain the effect with energy transfer: the electrons in the conductors are the carriers of the energy. As energy flows through the materials, the temperature gradient causes a flow of electrons in a certain direction (depends on the character of the material), and thus an electrical current can be observed. By applying an electrical current through the materials, the electrons move in the negative direction of the electric field, and as the electrons are the carriers of the energy, the side that the electrons move towards is heated, and on the contrary, the other side is cooled.

Although the thermoelectric phenomenon was observed in the early 19^{th} century, the devices that could make use of this effect were not manufactured for many years. It was not until the mid-20^{th} century that the first practical application for a thermoelectric device was put into use (Tellurex, 2010). With the development of modern science and technology,

especially in electronics and energy, the world stepped into the 21st century. Meanwhile, our daily life largely relies on electronic devices and transportation systems, and the main problem of these is that they not only require a lot of energy to function, but have to dissipate heat they generate into the surroundings. As scientists are working to develop devices to conserve energy, thermoelectric devices can be an excellent choice to provide cooling for the electronic devices and at the same time make use of the energy that is now wasted in the form of heat. With the heat dissipated, the thermoelectric modules would be able to generate direct current (DC) electricity out of it, and the DC output can be stored and redistributed to other electric devices. Thus the efficiency of the whole electronic device would be increased and the working environment for the device would be cooled down to a more appropriate temperature.

The most common thermoelectric module is shown as Fig. 1-1. The module is composed of three parts; the upper and lower plates are made of ceramic while the pellets contain two kinds of bismuth telluride semiconductors, N-type (refers to negative) and P-type (refers to positive).

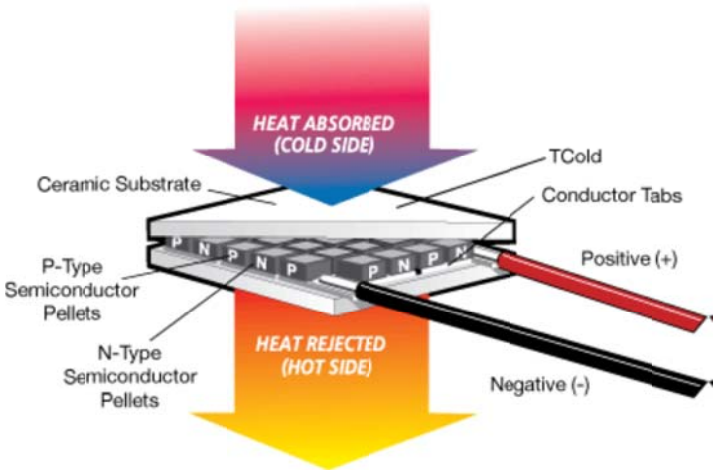

Figure 1-1 Components of Thermoelectric Module (Tellurex, 2010)

For the P-type semiconductor, as electrons diffuse away from the holes in the material, the material creates an abundance of holes. In the P-type semiconductor the holes are regarded as the majority charge carrier and thus the P-type material behaves as the positive charge element in the module. On the contrary, the N-type material shows a character that the holes are considered as the minority carriers, which means the N-type semiconductor is the negative element in the module. The N-type pellets and P-type pellets are connected in series to make sure that with the flow of direct current the module would be cooled on one side and heated on the other side.

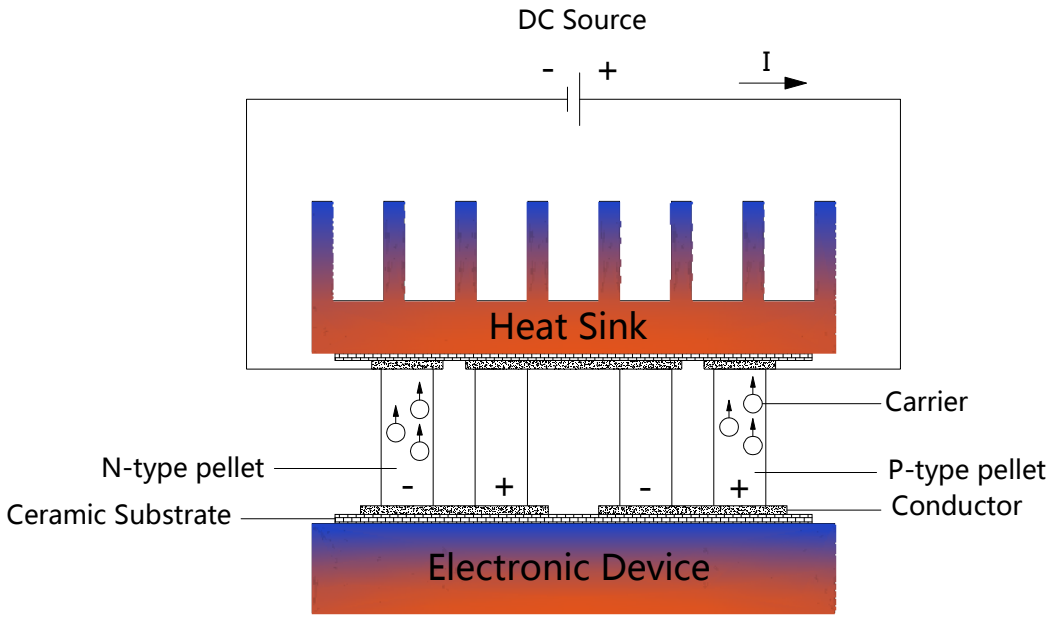

Figure 1-2 Working Principle of Thermoelectric Module (Tellurex, 2010)

Figure 1-2 shows a typical utilization of a thermoelectric module, which is providing cooling to some kind of electronic device (e.g. CPU, GPU). As the thermoelectric device does not need any rotating components or space for vaporization for a working liquid, it is relatively easy to maintain the module and it can be very reliable. As a consequence, thermoelectric modules can be used in places that require minimum space and deliver a stable cooling effect while in a vibrating or sensitive environment, or in other places that are not convenient for a refrigerant-based cooling system (e.g. a conventional vapor-compression refrigeration system).

Thermoelectric devices can not only be used as a heating/cooling device, but can also be utilized in power generation. As shown in Fig.1-3, with a heat resource and a heat sink, thermoelectric devices can be used to generate direct current and thus power electric equipment.

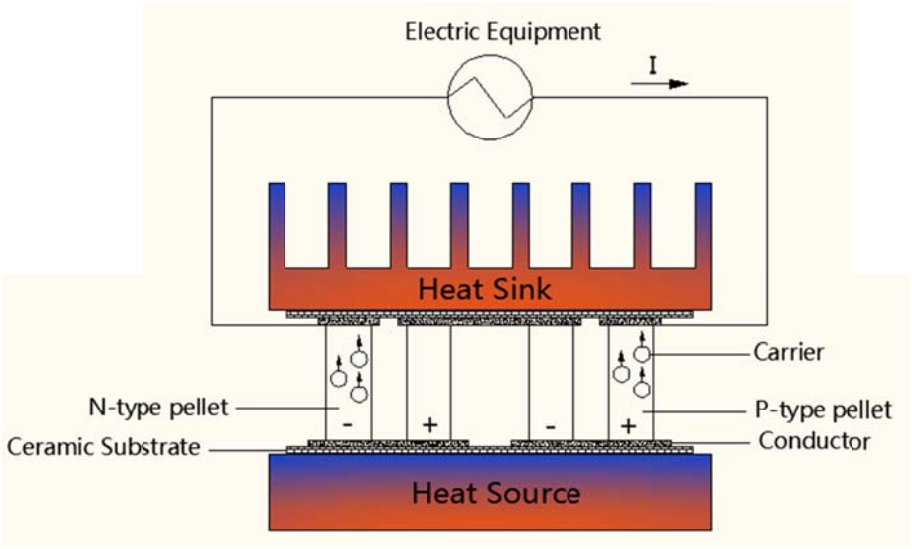

Figure 1-3 Working Principle of Thermoelectric Generator (Tellurex, 2010)

Although a great deal of research has been done on the thermoelectric character of solid semiconductors, to our knowledge seldom has research focused on a fluid that could display thermoelectric properties. If the result of a nanoparticles and fluid mixture show the same characteristics as solid thermoelectrics do, the fluid thermoelectric material may have certain benefits over the solid. First of all, the fluid itself can be more flexible than a solid with regards to geometry; secondly, with proper design of the containers or tubes that contain the fluid, it would likely be easier to achieve efficient heat transfer between the thermoelectric fluid and the heat source/sink, compared with a solid thermoelectric element. Last, but not least, for replacement the refill of the fluid may be easier than to replace the solid modules, resulting in a shorter time to fix the module when necessary.

This thesis mainly focuses on the characteristics of a nanofluid that is composed of nanoparticles exhibiting some Seebeck coefficient and DI (de-ionized) water, with some surfactant added to it. The following chapters are included in this thesis: Chapter 2 consists of a literature review of thermoelectric materials and nanofluid heat transfer properties, including the characteristics of the most commonly used semiconductor thermoelectric material, bismuth telluride and multiwall carbon nano tubes; Chapter 3 covers the introduction of the design, equipment and methodology used in the experiment process; Chapter 4 presents the research and analysis of the thermoelectric phenomena observed in the experiments; Chapter 5 presents the thermophoresis effect exhibited by an NaCl solution; Chapter 6 performs the detailed analysis and comparison between the experimental data and the theoretical results; and finally, possible applications of a thermoelectric nanofluid and conclusions for the entire thesis are given in Chapter 7, as well as recommendations for future work.

CHAPTER 2 LITERATURE REVIEW OF THERMOELECTRIC MATERIALS

A. Thermoelectric properties of bismuth telluride

Bismuth telluride is one of the most commonly used thermoelectric materials at room temperature, with a Seebeck coefficient of -150 μV/°C and an electrical resistivity of 4×10^{-5} Ω m at room temperature. The Seebeck coefficient can reach up to -287μV/°C at 54 °C, and also depends on the thickness of the bismuth telluride film (Tan, et al., 2005).

Several characteristic parameters are required for evaluating a thermoelectric material: the Seebeck coefficient, which represents the potential of converting thermal energy into electricity; the electrical resistivity/conductivity, which represents the ability to conduct electricity, and the thermal conductivity, which indicates the ability to conduct heat through the material. In order to evaluate the effectiveness of thermoelectric materials, the dimensionless thermoelectric figure of merit *ZT* is introduced in the following equations (DiSalvo, 1999):

$$ZT = \frac{TS^2}{\rho\lambda}, \qquad \text{[Eq. 2-1]}$$

$$\text{Or} \quad Z = \frac{\sigma S^2}{\lambda}, \qquad \text{[Eq. 2-2]}$$

In which,

$$\rho = \frac{1}{\sigma} \qquad \text{[Eq. 2-3]}$$

where T is the temperature (°C), S the Seebeck coefficient (μV/ °C), ρ the electrical resistivity (Ω·m), σ the electrical conductivity ($S \cdot m^{-1}$), and λ the thermal conductivity ($W\,m^{-1}\,°C^{-1}$). The T in equation (1) is multiplied on both sides of the equation in order to convert the Z into a nondimensional variable.

A material with greater ZT would be more suitable to be a thermoelectric material. Usually, a material with ZT of 1 could be regarded as a good one and the most up-to-date ZT values range from 2.5 to 3 (Walter, 2007). For a thermoelectric cooler (TEC), a larger ZT would lead to a higher COP (Terry Hendricks, 2006). As Eq. 2-1 shows, in order to get a relatively large ZT, S needs to be as large as possible while ρ and λ should be minimized.

B. The Seebeck coefficient of bismuth telluride

The Seebeck coefficient and electric conductivity of bismuth telluride (Bi_2Te_3) thin films is related to both the thickness of the films and the temperature (Tan, 2005). Sine here Bi_2Te_3 is used in the form of nanoparticles, potential size effects on their S values are of interest.

By sputtering Bi_2Te_3 onto a 7.5cm by 2.5 cm glass slide, the thin films were deposited, with the thickness of the films being proportional to the sputtering time (Tan, 2005).

Figure 2-1 shows that *S* for Bi_2Te_3 depends on the film thickness (Tan, 2005). It was observed by the author, however, that the thickness of the film is not proportional to S. Although the peak of the Seebeck coefficient is observed at 54°C for the 9.8-μm-thick film, the curves of the three films with different thicknesses are not similar. They even cross each other at some points. Figure 2-1 indicates that the thickness of the bismuth telluride thin film is affecting the result somehow. But there is an optimum thickness and temperature for the highest possible value of the Seebeck coefficient.

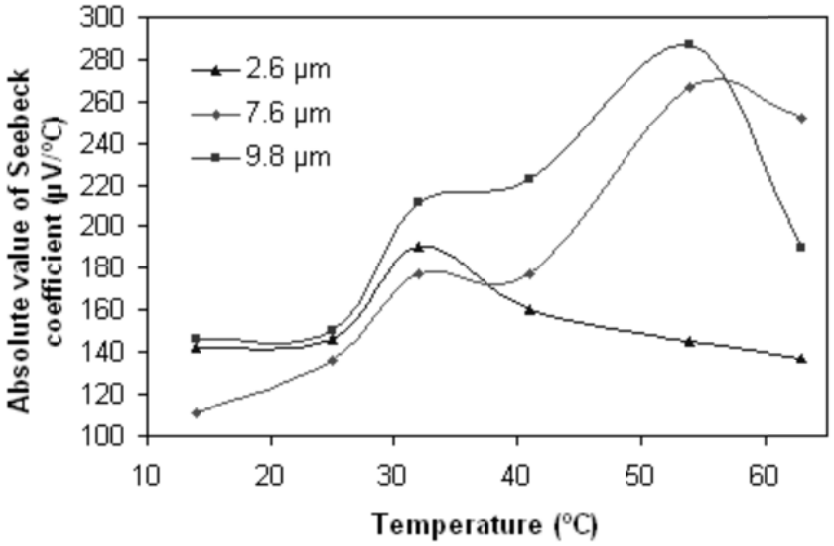

Figure 2-1 Seebeck coefficient for Different Thickness of Bi_2Te_3 Films (Tan, et al., 2005)

Since Fig. 2-1 shows the absolute value of *S*, the largest Seebeck coefficient is actually -287μV/°C at 54 °C for the 9.8-μm-thick film.

For the electrical resistivity, due to the difference of cross-sectional area, not surprisingly thicker films have a relatively small electrical

resistivity and the thinner ones have a larger one, as shown in Fig. 2-2. Meanwhile, the electrical resistivity is itself a function of temperature. For the 2.6-μm film, the electrical resistivity decreased with increasing temperature while on the contrary, the 9.8-μm film's electrical resistivity reached a peak at 40°C and dropped after that (Tan, 2005).

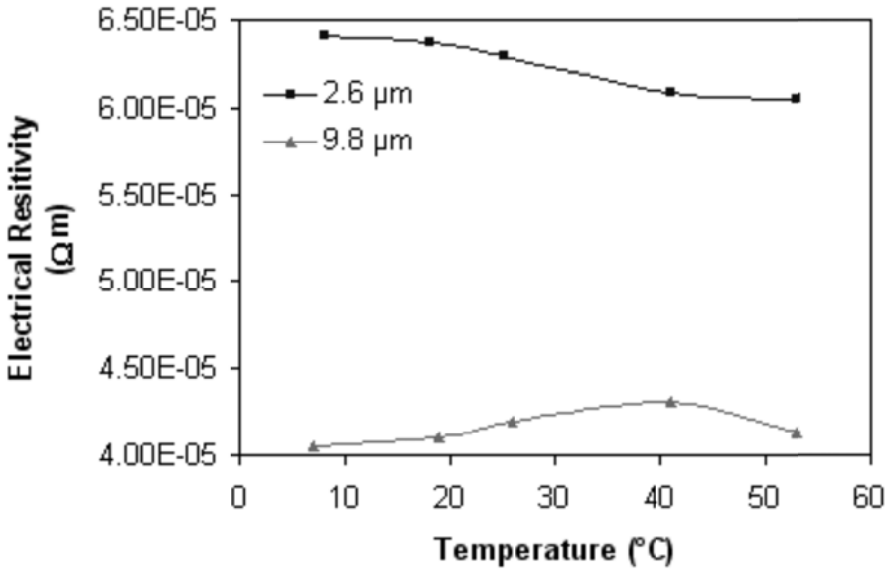

Figure 2-2 Electrical Resistivity of Different Film Thickness

(Tan, et al., 2005)

The paper also presented some SEM (Scanning Electron Microscope) images of films for different thicknesses. The grain size for 2.6μm, 4.5μm and 9.8μm were correspondingly 900nm, 1000nm and 1500nm, which suggested that with longer sputtering time, the grain size became larger (Tan, et al., 2005)

.

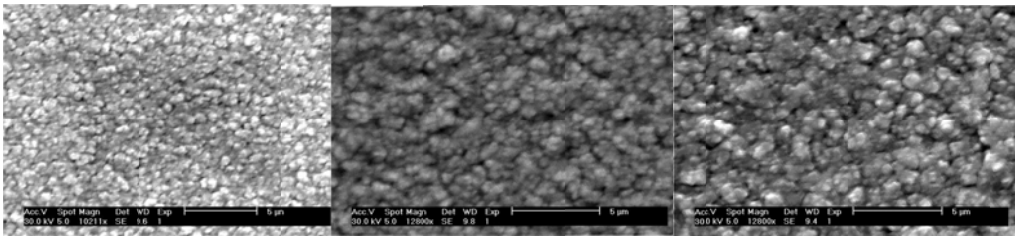

Figure 2-3 SEM Micrographs for 2.6MM, 4.5MM and 9.8MM Films

(Tan, et al., 2005)

C. Solution for stable nanofluid suspension

Due to the character of different nanoparticles, the particles may agglomerate while mixed with water to form a nanofluid. In order to maintain well-distributed nanoparticles in the fluid, there are two traditional ways to do it: one is to use an ultrasonicator to break up the aggregates and the other way is to add surfactant to the solution to make it stable for a relatively long period (Huaqing Xie, 2003). The former approach may not provide a long-term stable suspension, while the latter way would not be able to dissipate particles so well in the suspension. In the paper of Huaqing Xie and Hohyun Lee, with boil and reflux in nitric acid and nitric/sulfuric acid mixture, after being diluted by distilled water, filtered, and washed repeatedly till no acidity shown, the suspension of multi-walled carbon nanotubes (MWCNT) would remain stable for over 2 months (Huaqing Xie, 2003). In experiments, it is usually suggested that both methods be used to obtain a homogeneous and stable suspension.

CHAPTER 3 EXPERIMENTAL DESIGN AND SETUP

A. Materials used for the experiment

In order to test the thermoelectric character of nanoparticles, the experiment used three different kinds of nanoparticles: multiwall carbon nanotubes (CNT), aluminum oxide (Al_2O_3) nanoparticles and bismuth (III) telluride (Bi_2Te_3) nano powder. Of which, the CNT is a material with high electric conductivity and thermal conductivity, and at the same time, CNT does exhibit a Seebeck coefficient.

a. Multi-walled carbon nano tubes

The theoretical structure and transmission electron microscopy (TEM) of multi-walled carbon nano tubes (MWCNT) are shown in Fig. 3-1 (Reilly, 2007). The multi-walled carbon nano tube samples used in this experiment were synthesized by the MER Corporation, the product was produced without catalysts and there are 8-30 layers, with 6-20 nm in diameter (the whole layer) and 1-5 μm in length (the whole layer), and the density is 0.7g/ml. Due to the character of carbon nano tubes, it is essential to add some surfactant into the solution and ultrasonicate before the experiment.

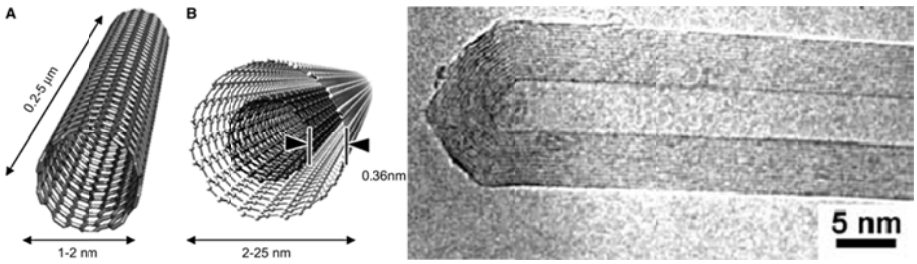

Figure 3-1 Theoretical Structure and TEM Images of MWCNT

(Reilly, 2007)

On top of adding surfactant and ultrasonication, adding acid or ethylene glycol could also work for a longer and stable solution (Huaqing Xie, 2003). In the experiment, solution with volume fraction of 1.0% for both the CNT and surfactant is used to test the character of the nanofluid.

b. Aluminum oxide nanoparticles

Aluminum oxide (Al_2O_3) is usually regarded as an electrical insulator, but with a relatively high thermal conductivity of 30 $W \cdot m^{-1} \cdot C^{-1}$ (Aluminum Oxide, 2010).

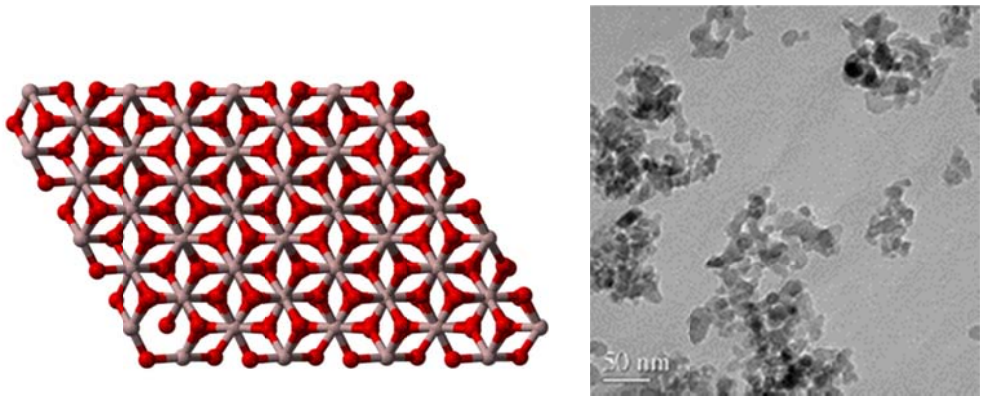

Figure 3-2 Theoretical Structure of Al_2O_3 (Mills, 2008)

and as-sprayed Al_2O_3 nano-particles under TEM (A.I.Y. Tok, 2009)

Figure 3-2 shows a theoretical structure of Al_2O_3 and as-sprayed nanoparticles under TEM (Transmission Electron Microscope). It was found in the current experiments that the nanoparticles do not agglomerate as fast as CNT during the experimental process, and thus surfactant was not required. Nevertheless, in order to unify the suspension and eliminate extraneous factors, surfactant with the same volume fraction is added to the suspension. In the experiment, solution with volume fractions of 0.5%, 0.75% and 1.0% were used to test the thermoelectric characteristics of the nanofluid.

c. Bismuth telluride nanoparticles

Bismuth telluride (Bi_2Te_3), a semiconductor is usually regarded as a typical representative of a thermoelectric material. It is one of the most efficient thermoelectric materials for refrigeration, and has a Seebeck coefficient between -224 μV/K at 298K (O. YAMASHITA, 2004). Figure 3-3 presents the theoretical structure of bismuth telluride (Materialscientist, 2009).

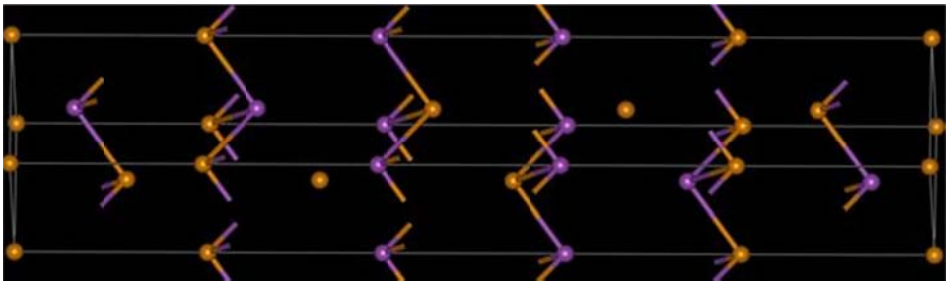

Figure 3-3 Theoretical Structure of Bismuth Telluride

(Materialscientist, 2009)

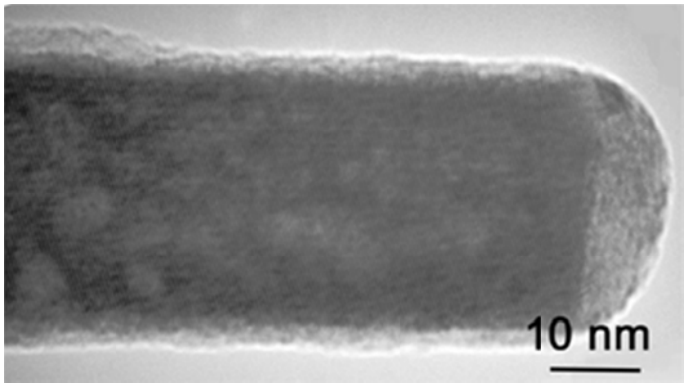

Figure 3-4 TEM Image of Bismuth Telluride Nano Rod

(A. Purkayastha, 2006)

Figure 3-4 presents a TEM image of bismuth telluride nano rod, with a reference line of 10 nm (A. Purkayastha, 2006). One aspect about thermoelectric materials in general is that the Seebeck coefficient does not maintain a stable value but can vary according to temperature. For example, the Seebeck coefficient of bismuth telluride reaches a peak at a value of -287μV/°C at 54°C (Tan, 2005). Similar phenomena occur for other kinds of materials, regardless of the electric conductivity and thermal conductivity.

B. Equipment used for the experiment

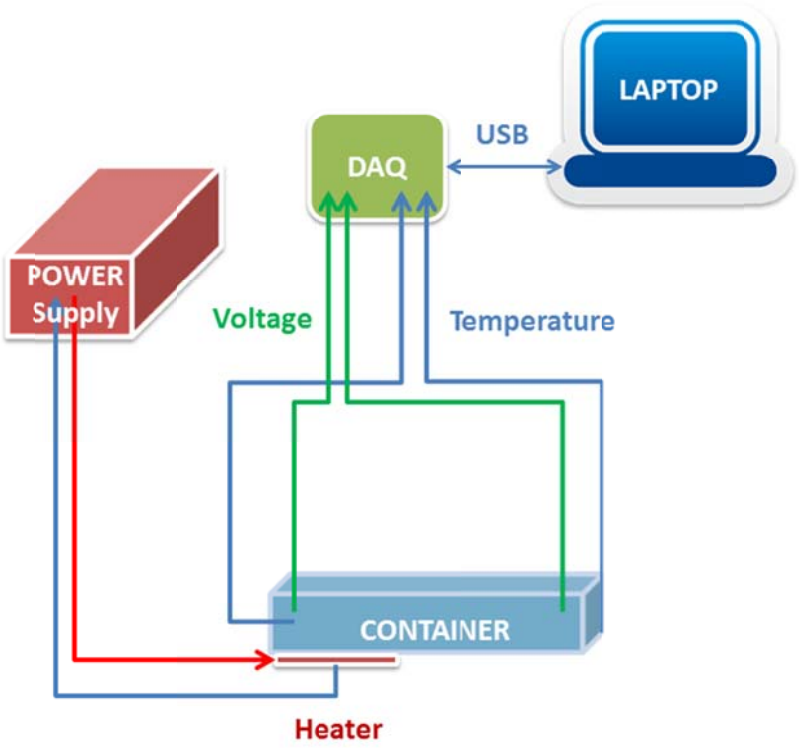

Figure 3-5 Diagram of the Experimental System

The whole system consists of five components, according to Fig. 3-5:

1. Container

   The container made from thin glass slides makes it relatively easy to transfer the heat from the bottom of the container to the fluid while at the same time, making it possible to observe through the transparent container.

2. Power supply

   The power supply is used to supply adjustable electric current through the heater to generate a stable thermal gradient along the container.

With a stable current, a smooth curve during the heating process is achievable.

3. Heater

   Since only heat is provided to the container, there are two kinds of heaters that can be used for this experiment. One is an electric film heater; the other is a P/N thermoelectric heater/cooler.

4. DAQ

   DAQ refer to 'Data Acquisition' system. The DAQ can be any kind of system that can transfer electric signals to the I/O signal and communicate with computer. The DAQ used in this experiment included an NI (National Instrument) module and Campbell Scientific modules.

5. Laptop Computer

   The computer used is a Dell INSPIRON 6400 laptop. A USB to VGA cable connects the laptop to the Campbell Scientific data logger which is finally used for the data acquisition.

a. Container for the nanofluid

1. Container used for the first round of experiments

The container for the nanofluid is hand made from microscope glass slides. The dimensions of the container are 150mm×25mm×25mm and at the end of the container, two glass slides are used as handles. Figure 3-6 presents a brief look of the container and the insulation attached.

As the container is made of microscope glass slides, the dimension of which is 75mm×25mm for each slide, in order to form a container 150mm long, two slides need to be bonded together. After each experiment, the container needs to be cleaned thoroughly by 70% alcohol. The adhesive used for the adherence of glass slides is made of organic material and thus can be corrupted by the alcohol. Due to the long term experiment, the adhesive can no longer seal the container, which means a new container needed to be built after about 6 months of experiments.

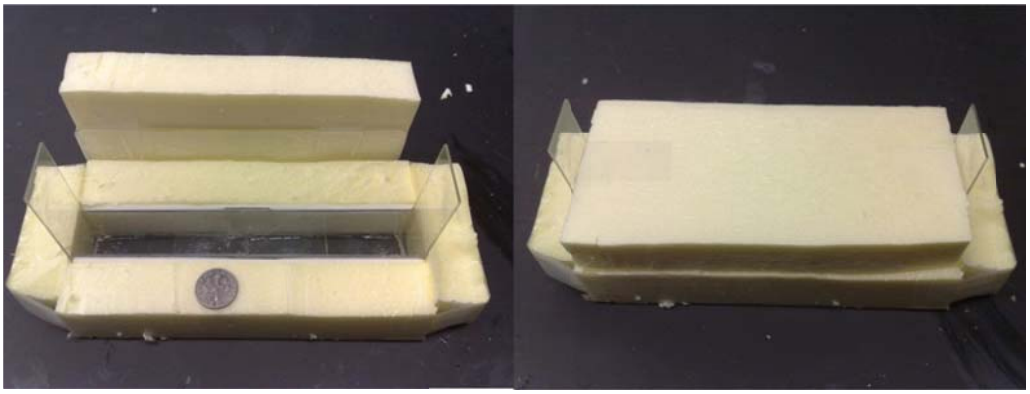

Figure 3-6 Image of First Container with Insulation (Penny as Reference)

2. Container used for the second round of experiments

As Fig. 3-7 shows, the second container is made of four 150mm×25mm×2mm ones and two 25mm×25mm×2mm glass slices. Five of them form a container while the last one is used as a cover.

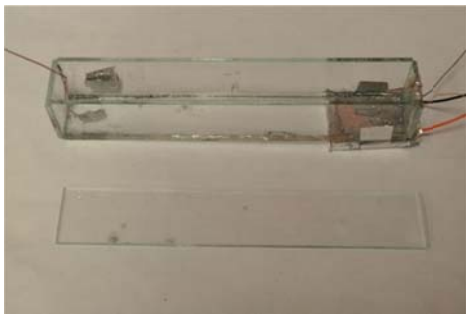

Figure 3-7 Container for the Second Round of Experiments

In order to eliminate the evaporation during the heating process, which would lead to the volume fraction change of the suspension, a glass cover is utilized to minimize the evaporation of the fluid and thus maintain the suspension at a stable situation.

b. Heating Equipment

Two thermoelectric heater/coolers are used to control the temperature on both sides of the container. Nevertheless, as mentioned in the utilization of the thermoelectric cooler part, the heat generated by the hot side of the thermoelectric cooler has to be removed continuously. Otherwise, the cooling effect would be greatly affected. After a few trials, it is observed that even with only passive cooling on the other side, it is still possible to obtain a temperature difference of over 40 ℃. The P/N

thermoelectric heater heats on one side and cools on the other side. If a greater temperature gradient is needed in the future research, two P/N thermoelectric heaters can be attached on both sides of the container while the heat generated on the cooling side needs to be removed in order to ensure a proper cooling effect. In this case, as shown in Fig. 3-8, instead of using a thermoelectric heater, an ordinary electric film heater is used to heat one end of the container and the other end is left in the ambient temperature for natural cooling. The electric film heater is attached to the outside surface of the container at the bottom, in case that the suspensions would corrupt the heater.

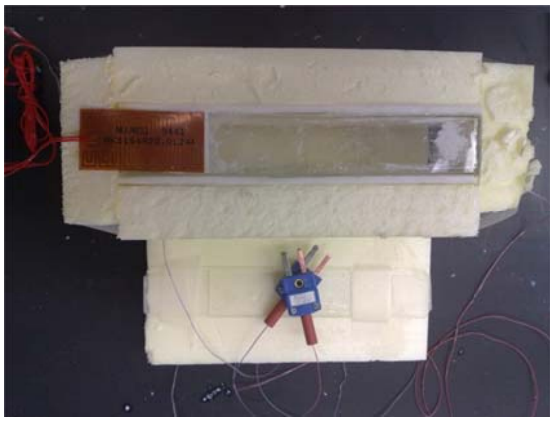

Figure 3-8 Container with Electric Heat at the Bottom (Reverse Side)

During the process of the experiment, some noises in the heating cycle are observed. It is either due to the electric current that flows through the electric film heater affecting the signal of the thermocouple, or the magnetic field that the electric current generated might have certain effect on the status of the nanoparticle suspension. As a solution, a thermoelectric heater is attached to the bottom of the container, with a

metal foil covered surface as a shield. With the modification, the noise during the heating cycle of the experiment is largely eliminated and the curve for the result appears to be much smoother.

In order to control the temperature of the heating process (the cooling process is natural cooling), Newport 3040 Temperature Controller is introduced (shown in Figure 3-9). The temperature controller is designed as a feed back system, with a current output port and a measurement port. With digital screen and button, the minimum adjustment for the controller is 0.01A. By controlling the output electric current to the electric heater, the heating cycle would be controlled easily. For the convenience of recording the temperature data with the computer, the built-in port for temperature measurement is not used and temperature is controlled manually.

Figure 3-9 Newport 3040 Temperature Controller (Newport, 2009)

c. Data collecting equipment

In the first few experiments, the main equipment used for the data collection was the DAQ (data acquisition equipment) SCXI-1300

manufactured by National Instrument, along with the desk top with a built-in DAQ port. Two different kinds of DAQ modules were used in data collection: SCXI-1100 and SCXI-1102 modules. SCXI-1100 module was used for the temperature signals, and the SCXI-1102 module was used for voltage signal collection.

According to the reply from NI engineer, the NI SCXI-1100 module has a phenomenon which is named as ‘ghost effect’. This effect indicates that if the module is measuring two different signals (like voltage and temperature) at the same time, one signal would very likely be identical to the other one, which is not the real signal. Due to this effect, the first set of data was largely affected by the ghost effect and the experimental equipment needed to be rebuilt with another kind of DAQ.

The Campbell Scientific CR23X was used as the DAQ for the redesigned system and there was no ‘ghost effect’ for this module, which indicated that the data collected would be reliable. As CR23X is not compatible with LabView, it was required that a specific control and monitoring software (PC200W, product of Campbell Scientific) be used to control the module and collect the data. The Campbell Scientific module records the data to the memory of itself and exchanges with the computer through a cable every time the user clicks the collect data bottom, which means it is not required to have a computer to control the data collection.

The probes for temperature measurement are T-type thermocouples, attached to the inner side of each end in the container with

thermal epoxy, which would not only enable a good heat transfer from the fluid to the thermocouple but also isolate the thermocouple from the surrounding that may affect its accuracy. Both probes for measuring the voltage are made of negative material of the thermocouple (copper-nickel/constantan), and are shielded with metal foil to eliminate the possible surrounding noise. A water bath tub is used to calibrate both thermocouples before they are attached to the container. Calibration is made in the range of 20℃ to 70℃, which is also the temperature gradient range of the experiment.

A multimeter is used to check the electric resistance of the fluid. The electric resistance of the mixtures of DI water and nanoparticles after ultrasonication is relatively high (over 10^6 Ω).

d. Other equipment used

In order to make certain mixture solutions of nanofluid, an electronic scale is used to measure the weight of the nanoparticles. The introduction of the electronic scale (shown in Figure 3-10) is to make sure that the volume fraction of the nanofluid is sufficiently accurate.

Figure 3-10 Mettler Toledo Electronic Scale

A syringe with division value of 1ml is used to specifically control the volume of the DI water added to the solution.

In order to record the PH value and electric conductivity of the nanoparticle suspension prepared, a PH meter and electric conductivity meter are used (shown in Figure 3-11). Calibrations are also needed for both meters before using them to measure the character of the nanofluid, and standard solutions for PH and electric conductivity are utilized. Usually the PH value is around 7 and the electrical conductivity is close to 0, which indicates that the resistivity is relatively large and the nanoparticle suspension can be regarded as an insulator.

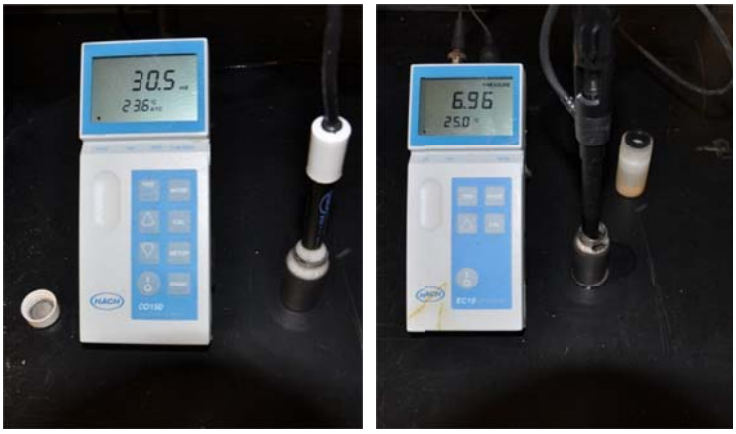

Figure 3-11 PH Meter and Electric Conductivity Meter

e. Software used for data collection and analysis

1. Campbell Scientific PC200W

Campbell Scientific CR23X data logger is used for data collection. Campbell Scientific PC200W 4.0.0.21 is used as special software for monitoring and importing the data. Figure 3-12 presents some basic information of PC200W software while Fig. 3-13 presents the software interface under different operating status.

Figure 3-12 Campbell Scientific PC200W Information

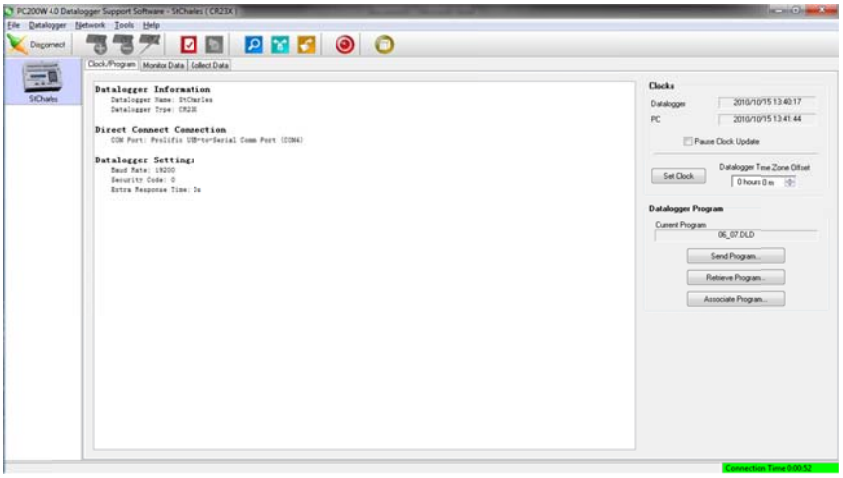

PC200W Main Interface

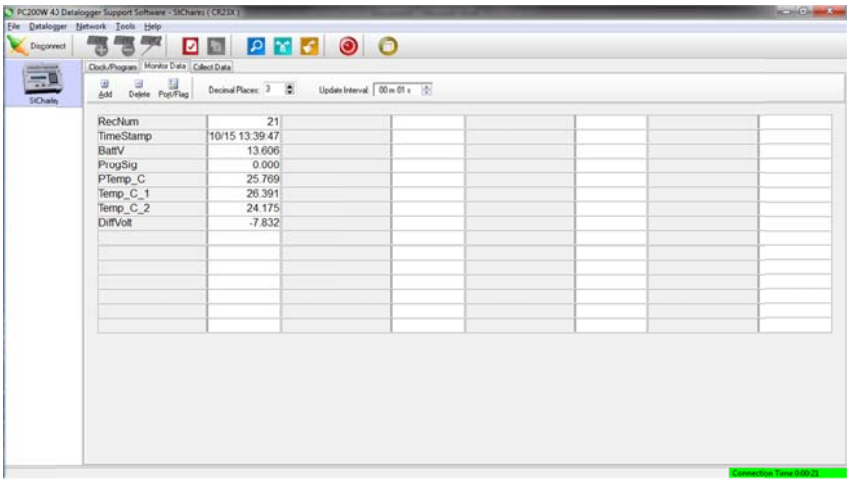

PC200W Monitor Interface

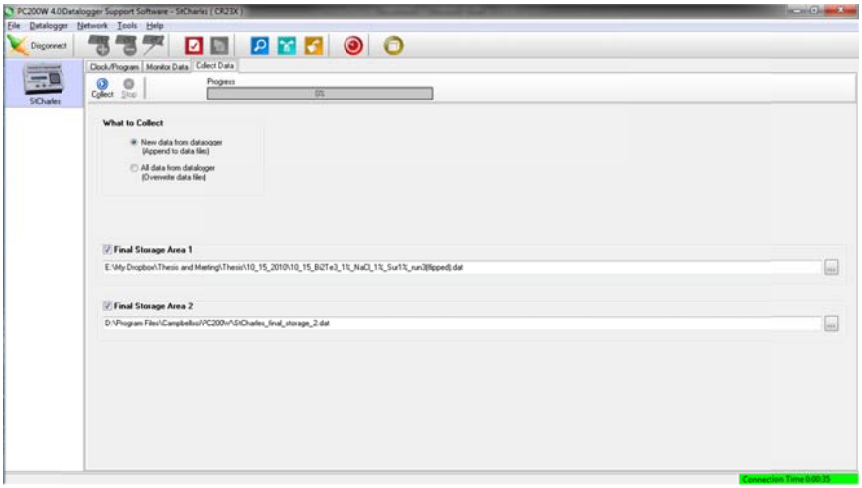

PC200W Data Collection Interface

Figure 3-13 PC200W Software Interfaces

2. Microsoft Excel

The data collected from CR-23X data logger include time, data logger reference temperature, hot end temperature, cold end temperature and voltage difference. In order to process the data much faster and clearer in Matlab, some pre-calculation can be made in Excel to achieve two parameters: temperature difference and Seebeck coefficient as Figure 3-14 shows.

	A	B	C	D	E	F	G	H	I	J
1	Order	Year	Date	Time	Reference Temp.	Hot End Temp.	Cold End Temp.	Voltage Diff.	Temp. Diff.	Seebeck Coefficient
2	0	2010	288	1200	24.72	23.35	23.42	-41.55	-0.07	593.5714286
3	1	2010	288	1200	24.72	23.35	23.43	-41.65	-0.08	520.625
4	2	2010	288	1200	24.72	23.35	23.42	-41.75	-0.07	596.4285714
5	3	2010	288	1200	24.72	23.35	23.43	-41.75	-0.08	521.875
6	4	2010	288	1200	24.72	23.35	23.43	-41.78	-0.08	522.25
7	5	2010	288	1200	24.72	23.34	23.42	-41.85	-0.08	523.125
8	6	2010	288	1200	24.72	23.34	23.42	-41.85	-0.08	523.125
9	7	2010	288	1200	24.72	23.34	23.42	-41.85	-0.08	523.125
10	8	2010	288	1200	24.72	23.34	23.42	-41.85	-0.08	523.125
11	9	2010	288	1200	24.72	23.34	23.42	-41.85	-0.08	523.125
12	10	2010	288	1200	24.72	23.34	23.42	-41.81	-0.08	522.625
13	11	2010	288	1200	24.72	23.34	23.42	-41.85	-0.08	523.125
14	12	2010	288	1200	24.72	23.33	23.42	-41.91	-0.09	465.6666667
15	13	2010	288	1200	24.72	23.33	23.4	-41.88	-0.07	598.2857143
16	14	2010	288	1200	24.72	23.33	23.42	-41.88	-0.09	465.3333333
17	15	2010	288	1200	24.72	23.34	23.42	-41.88	-0.08	523.5
18	16	2010	288	1200	24.72	23.33	23.41	-41.98	-0.08	524.75
19	17	2010	288	1200	24.72	23.33	23.41	-41.98	-0.08	524.75
20	18	2010	288	1200	24.72	23.32	23.41	-42.04	-0.09	467.1111111

Figure 3-14 Data Collected and Parameters Calculated in MS Excel

Nevertheless, the Microsoft Excel cannot process the data collected from Campbell Scientific CR-23X data logger, which is saved in a .dat file. As Excel cannot read the rows and columns in a .dat file, some modifications (using Matlab) need to be made before processing and save the data into a .txt file in Excel.

3. Matlab

The data collected from the data logger are analyzed with Matlab. Figure 3-15 shows the interface of Matlab while the pre-treatment of data is performed.

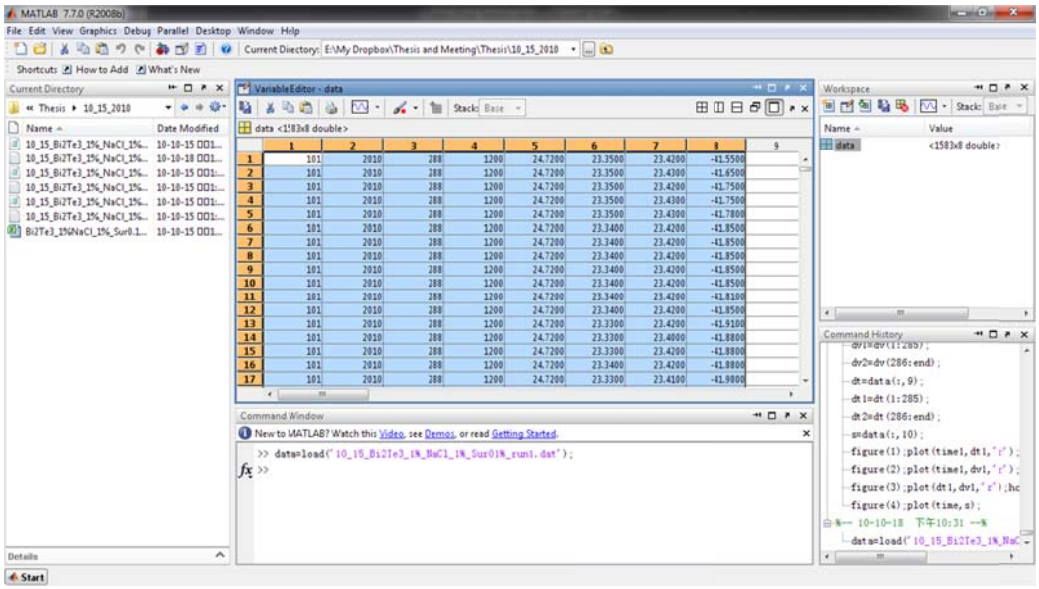

Figure 3-15 Matlab Interface Loading the Collected Data

First of all, the original data collected from the CR-23X data logger is in .dat files, change current directory to where the data file located. For example, on this computer, the directory is

'E:\My Dropbox\Thesis and Meeting\Thesis\10_15_2010' and user can use 'data=load('10_15_Bi2Te3_1%_NaCl_1%_Sur01%_run1.dat');' to load the data into Matlab matrix. Double click on the 'data' matrix in 'Workspace', copy the whole matrix and paste into Microsoft Excel for processing.

After processing by Excel, the data are analyzed in Matlab.

CHAPTER 4 EXPERIMENTAL TRIAL AND RESULTS

a. Performance Test for the Equipment

To make sure that the experimental equipment are functional and reliable, several trials should be performed before the actual nanofluid tests. Among which, sealing of the container, thermocouple calibration, contact of the thermocouple and test for copper wire and DI water (distilled water) are important ones.

1. Test for Sealing

Sealing of the container is of great importance in this experiment, since it is crucial to control the volume fraction. That means that there should not be any leaking in the container and a glass cover is included so as to eliminate the evaporation of the fluid.

Test for sealing is relatively easy compared to other tests. The container is first filled with DI water and placed on a paper towel, and then after waiting for half an hour see if there is any visible water mark on the paper towel. To be more specific, the container can be placed upon $CuSO_4$ powder, if the powder does not turn blue, that indicates that the container is properly sealed.

2. Thermocouple Calibration

The thermocouples used are T type thermocouples, which are designed to measure the temperature between -250°C to 350°C, with a sensitivity of 43μV/°C (Omega, 2010). The experiment is designed to perform in the range of room temperature (about 22°C) to 70°C and the

digital water bath can be used to calibrate the thermocouples. The temperature range of the water bath is from 0°C (with ice water mixture) to 100°C (with boiling water).

To calibrate the thermocouple, the water bath tub should be set to different temperatures, from 20°C to 70°C, with an interval of 5°C. The temperature of the water tub should be regarded as the reference temperature and the two thermocouple temperatures should be recorded and calibrated according to the different temperature interval.

3. Contact of Thermocouples

In order to make sure that the thermocouples are able to measure the temperature while electrically insulated from the fluid, thermal epoxy is introduced to maintain proper thermal conductivity and act as electric insulator; another crucial function of the epoxy is to properly attach the thermocouples at the bottom of the container.

To test the contact of thermocouples, a computer with certain software and a hand-held infrared temperature thermometer are needed. First run the software and monitor the temperature data acquired from the two thermocouples attached to the bottom and compare with the temperature readings of the inferred thermometer. Minor differences indicate that the thermocouples are in a good contact with the container.

b. Verification Test for Copper Wire

In order to verify that the wires used to measure the voltage across nanofluid are functional, several trial tests were performed.

The wire for measuring the voltage across the fluid is from the negative material (copper-nickel) of the T type thermocouple, and the copper wire used for testing is from the positive material of the T Type thermocouple. In this way, a differential thermocouple is created; this differential thermocouple can be regarded as a T type thermocouple. We are able to compare the measured voltage with the data from the manufacturer's data base that indicates different voltage difference in response to various temperature differences.

Experimental Plan:

1. Use connected copper wire and simulated voltage curve and show the difference.
2. Wire marked by "+" is adhered to the hot end of the container and connect to the positive junction of the DAQ board; the other wire sticks to the cold end and is connected to the negative junction.
3. Attach a thermocouple on each end of the container.
4. Run the test for copper with and without temperature measurement to make sure the signals are not affecting each other.

Results

Theoretical estimation is made using the 'Revised Thermocouple Reference Tables' from Omega (Omega, 2010) and the equation is made to be:

$$\Delta V = S \times \Delta T$$

In which *S* is the Seebeck coefficient of T-Type thermocouples.

For T-Type thermocouples, *S* is approximately -0.04229 mV/℃.

So

$$\Delta V = S \times \Delta T = -0.04229 \Delta T$$

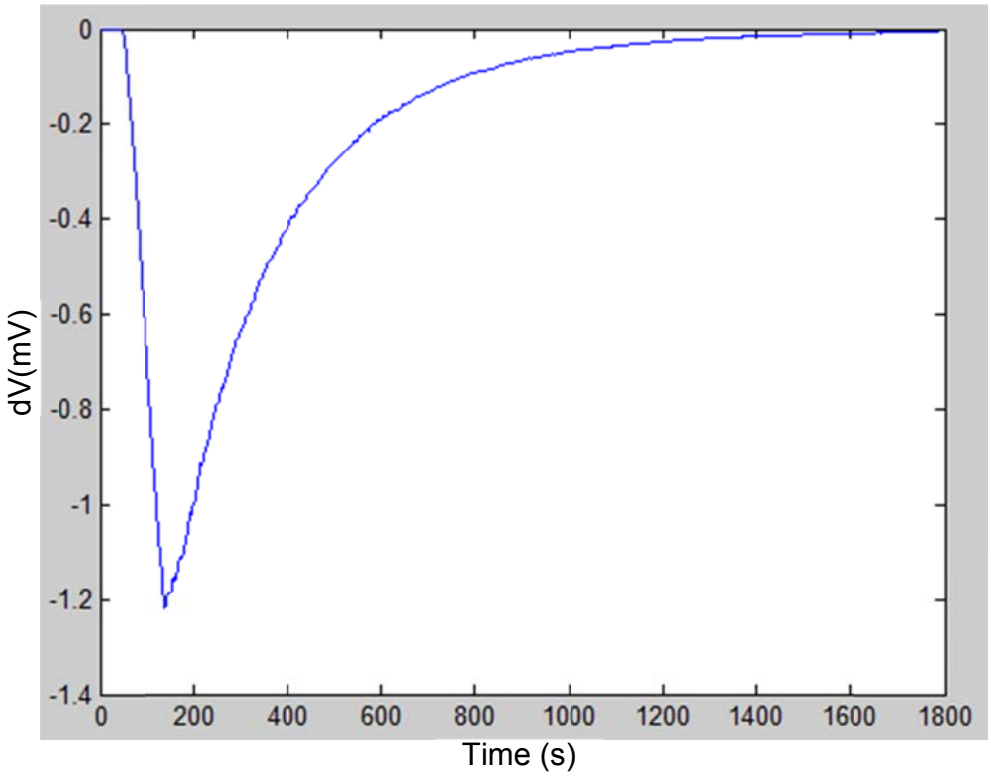

Figure 4-1 Copper Run without Temperature Measurement (4/22/2010)

Figure 4-1 is the verification test of the copper wire without the temperature measurement channel plugged in; it presents the voltage

change as a function of temperature difference. With only the voltage measurement channel plugged in, the curve is similar to the curve that both channels are plugged in and it is confirmed that there is no such 'ghost effect' on the Campbell Scientific CX23 module. The voltage measurement is accurate.

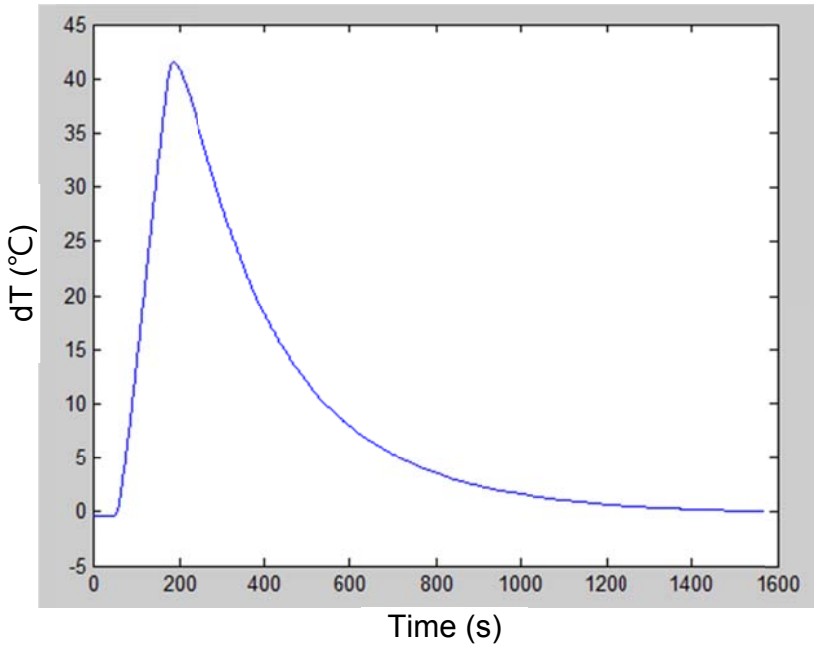

Figure 4-2 Copper Wire dT(℃) vs. Time(s)

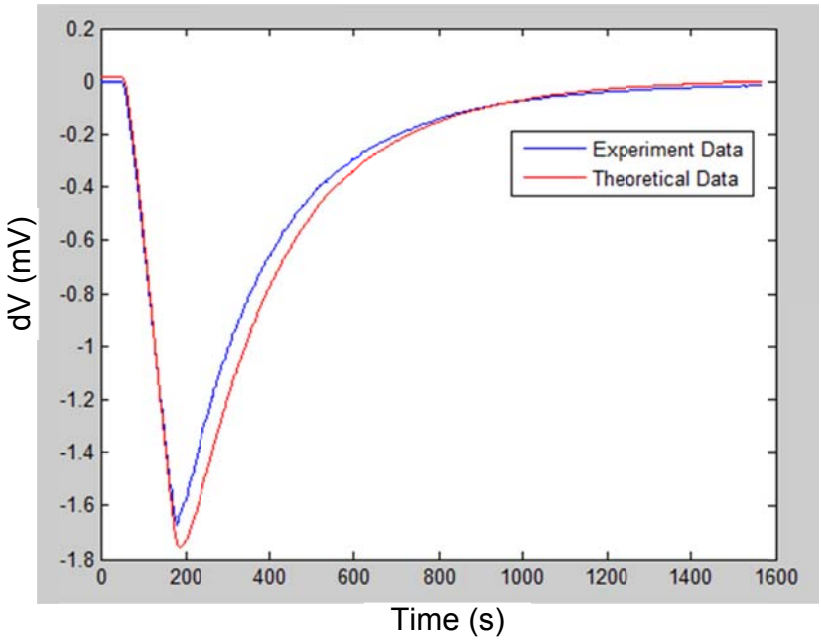

Figure 4-3 Copper Wire dV(mV) vs. time(s)

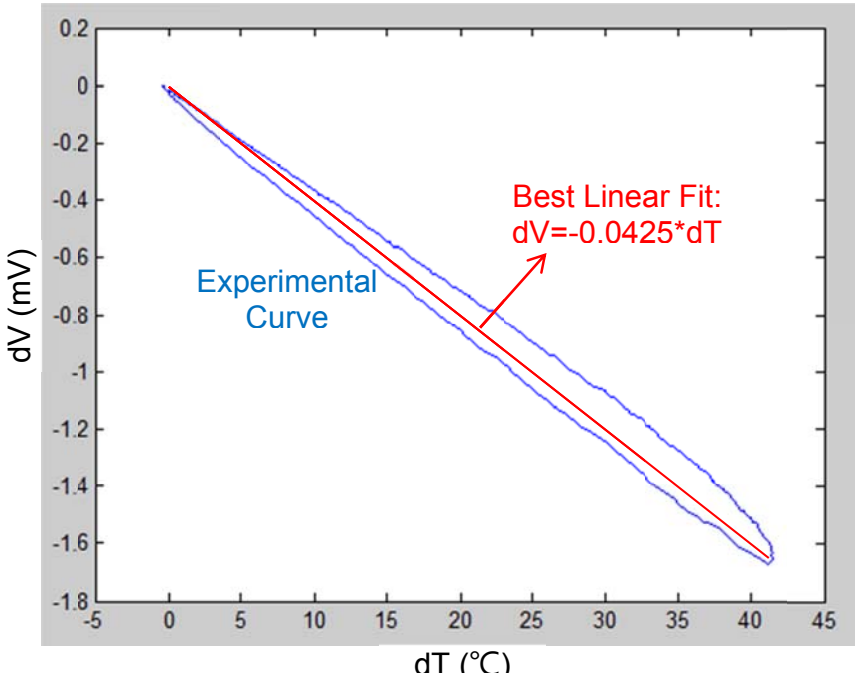

Figure 4-4 Copper Wire dV(mV) vs. dT(℃)

Figure 4-2 shows the temperature change with time with both temperature and voltage channels in use. The heating process lasts for

about 200 seconds and the container was naturally cooled after that. As Fig. 4-3 shows, the handbook data and the experimental data are close to each other, and so the experimental data can be regarded as accurate. There is another way to determine the Seebeck coefficient of the thermocouple composed by probes measuring the voltage and the copper: find a best linear fit in Fig. 4-4, and the slope (-0.0425 μV/℃) of the line is the *S* of this 'differential T-type 'thermocouple'. In this case, it is confirmed that the measurements for the temperature and voltage are accurate. The dV vs. dT curve also shows a good pattern that the Seebeck coefficient does not change much during the heating and cooling process and is a closed loop.

The next step is to test the fluid with electrolyte in it, thus increasing the electric conductivity of the fluid, and the observed phenomena will be discussed in Chapter 5.

CHAPTER 5 THEORETICAL BACKGROUND OF THERMOPHORESIS

One of the main differences between experiments of solids and fluids is the liquidity of fluids, which enables both conductive and convective heat, mass, and charge transfer. Although it is expected that some thermoelectric effects would be shown in the nanofluid, because of the Seebeck coefficient of the nanoparticles, the *thermophoresis effect* should also be taken into consideration.

Some studies showed that particles in a fluid can move due to a temperature gradient, which is normally regarded as *thermophoresis*, would be related to the thermoelectric effect in the fluid (Würger, 2009). For an external electric field of (Würger, 2009):

$$\mathrm{E}_{\infty} = \delta\alpha \frac{\mathrm{k_B}\nabla \mathrm{T}}{\mathrm{e}} \quad \text{[Eq. 5-1]}$$

where E_{∞} is the external electric field, $\delta\alpha$ the reduced Seebeck coefficient, $\nabla \mathrm{T}$ the temperature gradient and e the elementary charge. The external electric field generated by the temperature gradient is expressed in Eq. 5-1.

As the thermophoresis of the carriers in the solution would take place in a temperature gradient, a thermoelectric voltage would be formed accordingly (Sheng Zhang, 2004):

$$\Delta V_{te} = \frac{W_b}{2q} \ln\left(\frac{T_2}{T_1}\right) \approx \frac{W_b}{2qT} \quad \text{[Eq. 5-2]}$$

where $\Delta \mathrm{T} = \delta \cdot \mathrm{grad}(\mathrm{T}) = T_2 - T_1 \ll T_1$ and $\mathrm{V}(T_1) = 0$ and ΔV_{te} is the thermoelectric voltage, W_b the activation energy and q the charge of the ions.

For NaCl solutions at a temperature 25~75°C, the activation energy during dissolution is -43.54 kJ/mol (Sheng Zhang, 2004), and *q*=1. During the experiments reported in this thesis, the mean temperature was 45°C. Thus, the Seebeck coefficient of the NaCl solution is (Sheng Zhang, 2004):

$$\mathrm{S} = \frac{W_b}{2qT} = -483.8 \mu V/K$$

In this case, the maximum voltage due to thermophoresis of the only the NaCl solution would be:

$$\mathrm{V}_{MAX} = S \cdot \Delta \mathrm{T}_{MAX} = -483.8 \mu V/K \cdot 30K = -14.51 \mathrm{mV}$$

CHAPTER 6 NANOFLUID EXPERIMENTS

Before nanofluid experiments, a trial with no nanoparticles in the fluid was performed to verify that the voltage difference is due to the nanoparticles.

Since the suspension is designed to be heated on one end and naturally cooled on the other end, a thermal gradient is formed within the container. As NaCl was added to the suspension to reduce the noise, and nanoparticles were added to the DI water, it is highly possible that the thermal gradient would lead to some thermophoresis effect on the ions in the NaCl solution. Furthermore, as the particles would usually gain positive or negative charge, the thermophoresis effect would lead to an electric gradient and thus affect the voltage difference that is anticipated.

a. Experiment on solutions without nanoparticles

1. Components: 1%NaCl+1%Surfactant+DI Water (Positive)
2. Suspension characteristics:

   G=32.9μs pH=6.82
3. Conditioning:

   Process the solution in ultrasonicator for 15 to 30 minutes.
4. Procedure:

   4.1 Transport the solution from container used for ultrasonic conditioning to the glass channel used for experiment.

   4.2 Turn the power for DAQ and power supply on.

4.3 Open PC200W software on laptop, connect the USB to VGA cable, click on ‘connect’ bottom and wait for the software returning ‘connected’ instruction.

4.4 Turn on the power supply to heat the hot end of container until the temperature difference between the hot and cold end reaches 30°C. Turn off the power supply and wait for the fluid to naturally cool down to ambient temperature (the cold side does not have forced cooling but natural cooling).

4.5 When the temperature difference between the hot end and cold end dropped to 3°C, stop the DAQ and upload the data to computer.

4.6 Switch the probe for voltage measurement and perform the previous procedures again, and upload the data to the computer.

4.7 After the experiment, pour the nanoparticle suspension into a container and transport to labeled waste container, clean the container with 70% alcohol and pour the cleaning fluid into the waste container. Write the name of the components in the fluid on the tag of waste container (ex. ‘Carbon Nano Tubes’, ‘Alcohol’, etc.).

4.8 Make sure that all experiment equipment are in place, clean up the experimental station and shut down all equipment.

The nanoparticles used in the experiment include aluminum oxide (Al_2O_3), carbon nano tubes (CNT) and bismuth telluride (Bi_2Te_3).

Table 6-1 Parameters of NaCl Solution

Suspension	Volume Fraction	Weight	Water Volume
NaCl	1.00%	438.34 mg	20 mL
Surfactant	1.00%	202 mg	
pH	Electric Conductivity	Ultrasonicate Duration	
6.82	32.9μs	15 min	

Table 6-1shows the components in the NaCl solution that was used for the experiment. For all solutions and suspensions, the volume was 20 mL, with 1% volume fraction of surfactant and 1% volume fraction of NaCl. NaCl was added to the suspensions to eliminate the noise that occurred during the experiments.

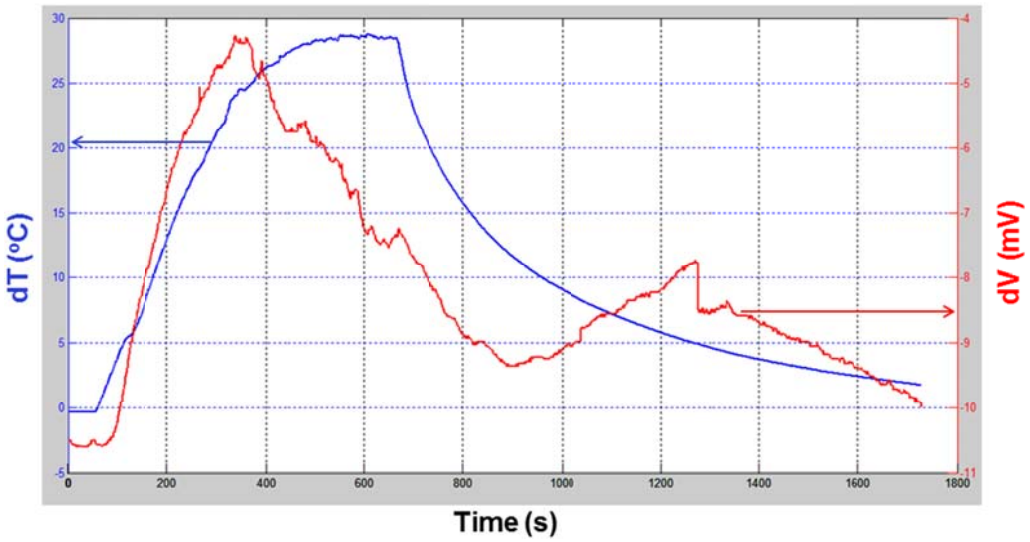

Figure 6-1 NaCl Solution dT and dV vs Time

In Fig. 6-1, dT and dV during the experiment of NaCl solution is shown in the same graph, where the blue line indicates the dT curve and the red line indicates the dV curve. The highest temperature difference (28°C)

occurred at around 700 s, at which point the power supply was turned off for natural cooling. The dV curve presented does not reach a peak at the same time, but shows a peak of 4 mV at 350s. As mentioned in Chapter 5, NaCl solution is expected to show a maximum dV of -14mV in the experiment (theoretically), and the maximum dV observed in this experiment was about -6mV.

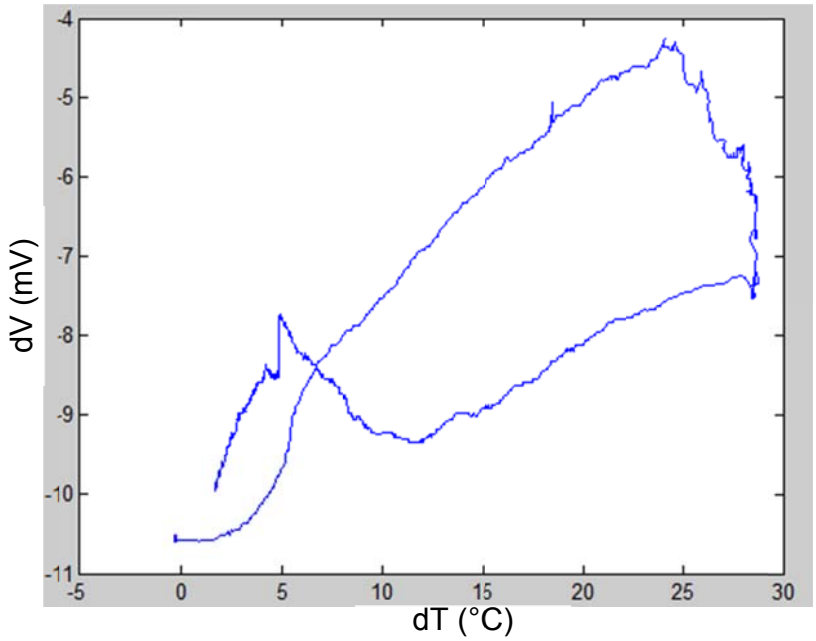

Figure 6-2 NaCl dV(mV) vs. dT(C)

Figure 6-2 shows the dV and dT relationship for the NaCl solution. The dV and dT plot does not imply that there is a direct linear correlation between dV and dT. In other words, the correlation of dV and dT for NaCl solution is not very strong.

b. Experiment on CNT suspension

Table 6-2 Parameters of CNT Suspension

Suspension	Volume Fraction	Weight	Water Volume
CNT	1.00%	142.45 mg	20 mL
NaCl	1.00%	438.14 mg	
Surfactant	1.00%	202 mg	

pH	Electric Conductivity	Ultrasonicate Duration	Manufacturer	Mesh Size
-	-	15 min	MER Corporation	-270 (<53μm)

Table 6-2 shows the parameters for the CNT suspension. In order to control the variables, the only difference between the CNT suspension and the previous NaCl solution used in the experiment is that 1% volume fraction of CNT nanoparticles were added to the suspension. Ultrasonication was used for mixing all the components and forms an evenly distributed suspension. pH and electric conductivity data were not obtained for the CNT suspension.

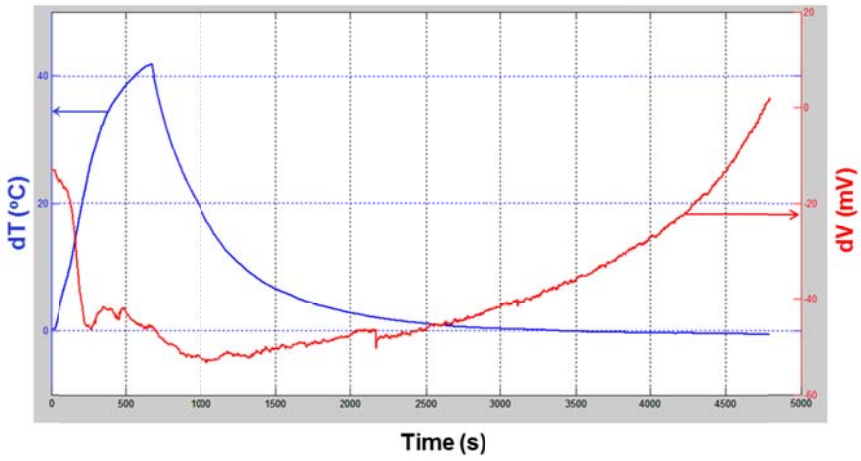

Figure 6-3 CNT dT and dV vs Time

The electric heater was shut off at 700s in Fig. 6-3, while the minimum value of dV for the CNT suspension was reached at 1000s, with a lag of 300s. The positive probe for voltage measurement was attached to the heated end of the container and the negative probe was attached to the cooled end. The CNT suspension shows a dV curve different from that of the NaCl solution, with the voltage difference measured dropping as the hot end is being heated.

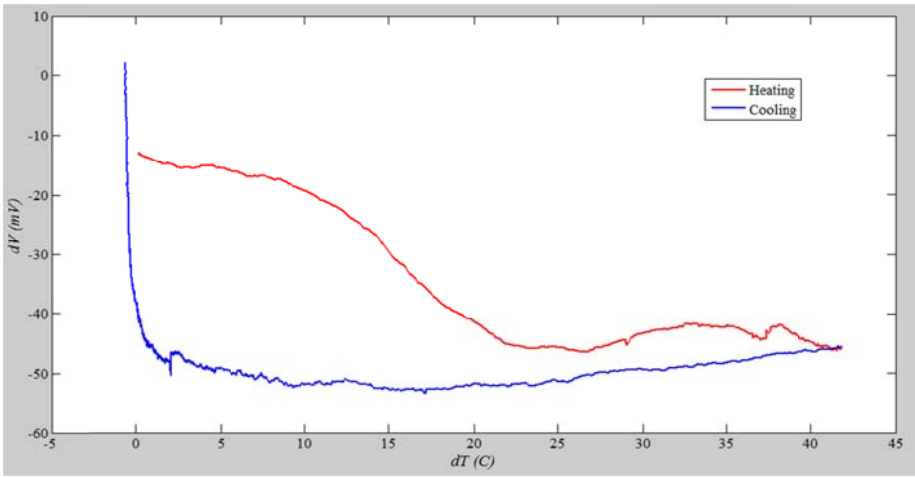

Figure 6-4 CNT dT vs. dV

Figure 6-4 presents the correlation of dV and dT for the CNT suspension. The heating process show a curve that is not proportional to temperature, while the cooling process shows almost no correlation between dV and dT. Bulk CNT is not a typical thermoelectric material, and it can be determined how much dT and dV are correlated in the CNT suspension by the analysis in the following part of this chapter.

c. Experiment on solution with Al_2O_3 nanoparticles

Table 6-3 Parameters of Al_2O_3 Suspension

Suspension	Volume Fraction	Weight	Water Volume
Al_2O_3	1.00%	81.4 mg	20 mL
NaCl	1.00%	434 mg	
Surfactant	1.00%	202 mg	

pH	Electric Conductivity	Ultrasonicate	Manufacturer	Grade
-	-	15 mins	Nanotechnologies, INC	50 nm

Table 6-3 contains the parameters of the Al_2O_3 suspension. Although the density of Al_2O_3 is not as large as other nanoparticles, and would be easier to achieve an evenly distributed suspension with a relatively short time of ultrasonication, the suspension was processed in the ultrasonicator for a same amount of time. pH and electric conductivity data were not obtained.

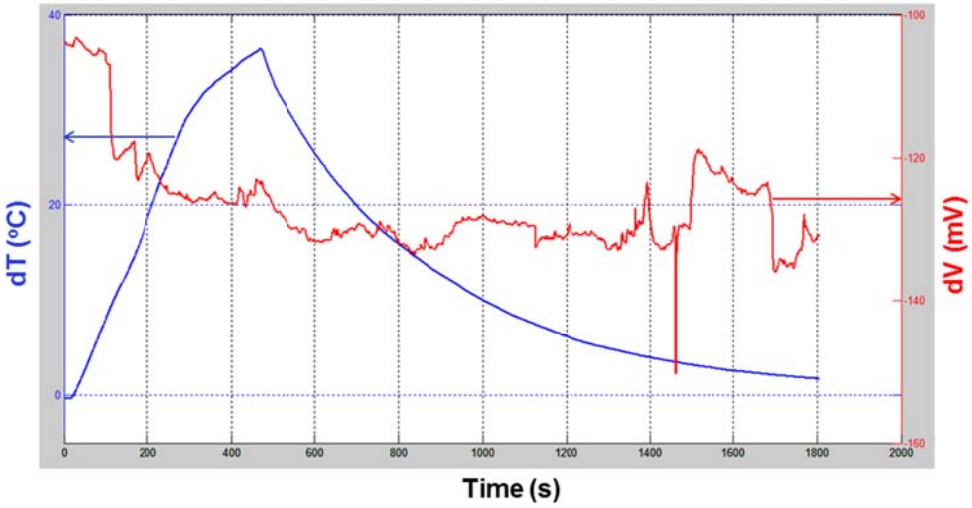

Figure 6-5 Al_2O_3 dT and dV vs Time

According to Fig. 6-5, the temperature difference curve for Al_2O_3 suspension does not show an obvious difference, compared with the dT curves for the NaCl solution and CNT suspension. On the other hand, the dV curve presented shows almost no direct correlation with the dT curve.

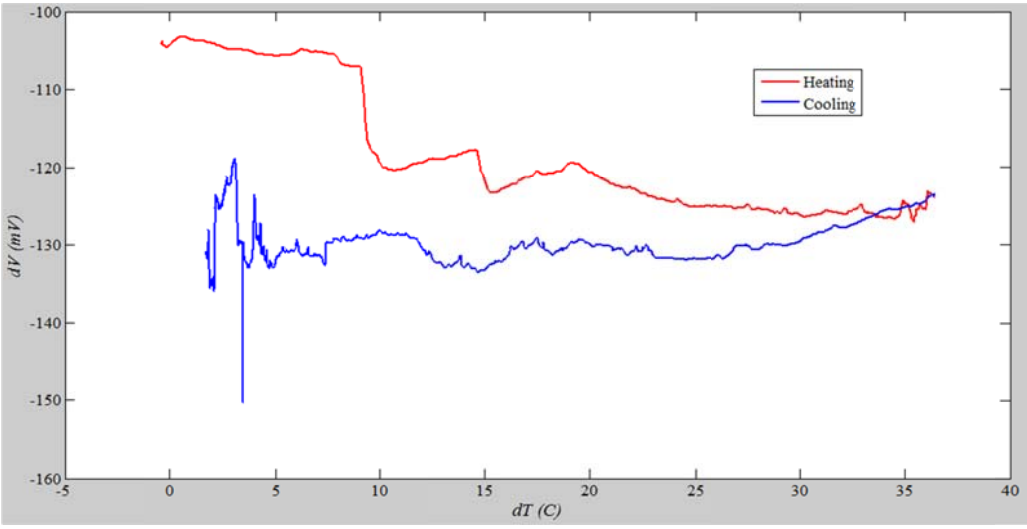

Figure 6-6 Al_2O_3 dT vs. dV

Figure 6-6 shows the curve of dT vs. dV for the Al_2O_3 suspension. In the curve, it is hard to see any correlation for dT and dV. For the heating process, the correlation between dT and dV is limited, and the dV is maintained at an average value of -125mV for the cooling process, which indicates that there's almost no thermoelectric characteristic shown by the Al_2O_3 suspension. Further discussion on the correlation is given in the least square analysis, to be presented later.

d. Experiment on Bi_2Te_3 nanoparticles suspension

Table 6-4 Parameters of Bi_2Te_3 Suspension

Solution	Volume Fraction	Weight	Water Volume
Bi_2Te_3	1.00%	1559 mg	20 mL
NaCl	1.00%	434 mg	
Surfactant	1.00%	202 mg	

pH	Electric Conductivity	Ultrasonication Duration	Manufacturer
6.96	30.7 μs	15 mins	American Elements

The parameters for the Bi_2Te_3 suspension are presented in Table 6-4. The pH value of Bi_2Te_3 suspension is almost neutral (close to 7), while the electric conductivity is close to the NaCl solution (32.9μs).

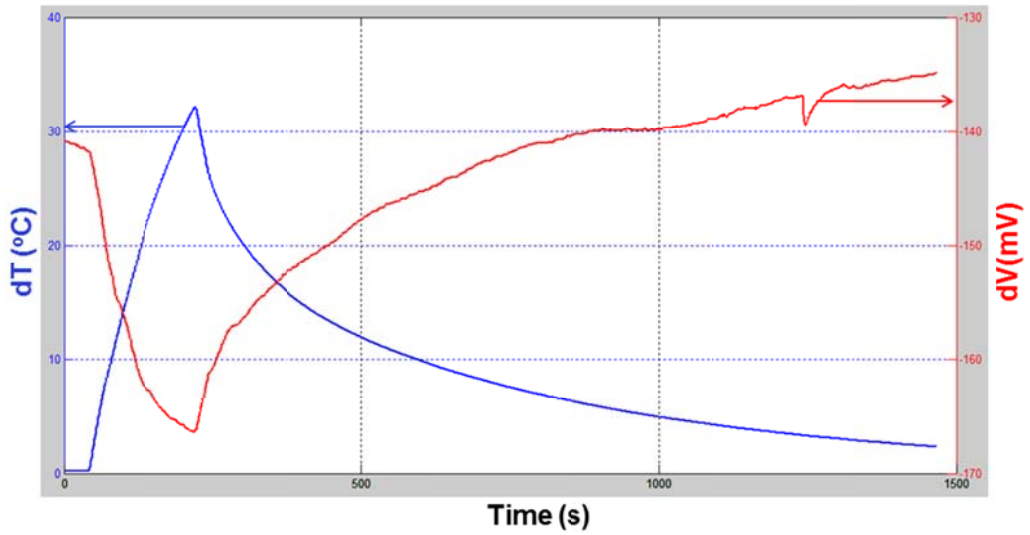

Figure 6-7 Bi_2Te_3 dT and dV vs Time

Fig. 6-7 presents the dT and dV curves for the Bi_2Te_3 suspension, which shows a very strong correlation for dT and dV. The maximum value of dT and the minimum value for dV were obtained at the same time (300s),

and there is an inverse proportional relationship between the two curves. As the Bi_2Te_3 is a typical thermoelectric material, it was anticipated that the Bi_2Te_3 suspension would accordingly exhibit a strong thermoelectric phenomenon.

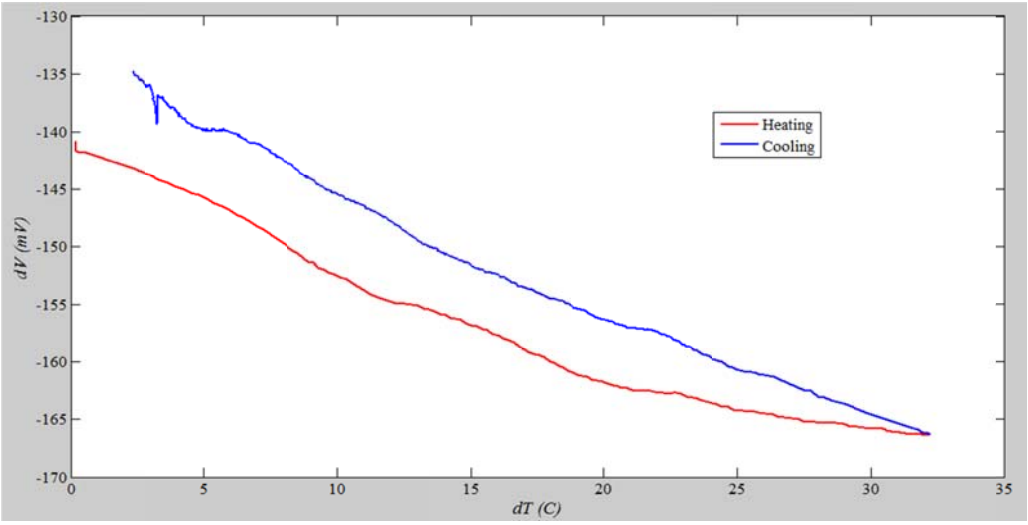

Figure 6-8 Bi_2Te_3 dT vs. dV

Figure 6-8 presents a clear correlation of dT and dV for the Bi_2Te_3 suspension. As shown in the figure, the curve is almost linear for both the heating and cooling processes. A specific correlation between dT and dV will be shown with further analysis in this chapter. A best linear fit can be utilized in order to find the 'Seebeck coefficient' for the Bi_2Te_3 suspension.

e. Data Analysis: Least Square Method

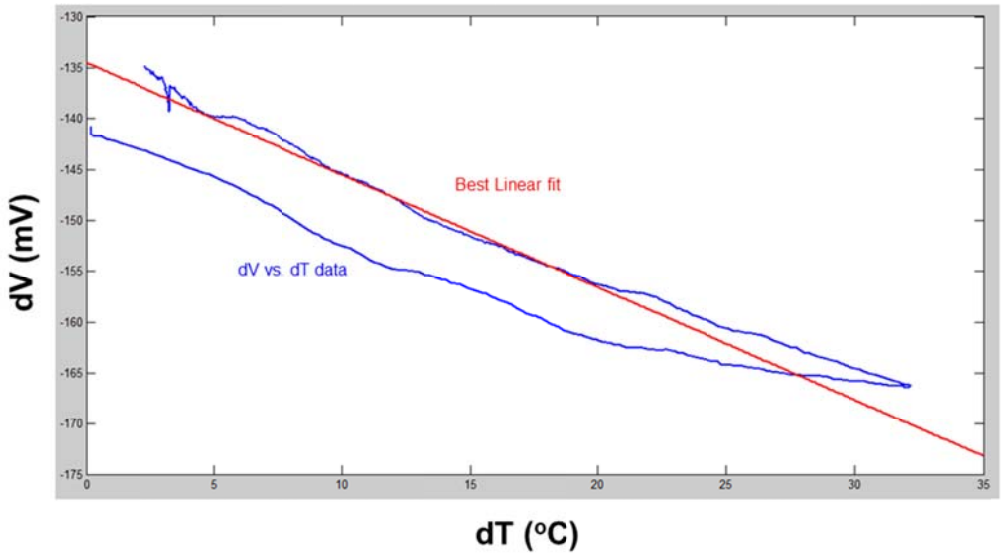

Figure 6-9 Least Squares Method for Bi_2Te_3 suspension

According to Fig. 6-9, there is a way to show whether there is any correlation between the temperature gradient and voltage difference. From the plots, it is shown that there is a relatively simple linear relationship between them. By employing the best linear fit, a correlation of dT and dV can be determined. In this case, there is no need to analyze the correlation for the two separate graphs showing ΔT vs. time and ΔV vs. time.

Due to the simple linear relationship between ΔT and ΔV, the least squares method can be used to decide the dependency of the two parameters.

A simple y=a+bx model can be used to identify the correlation of the two parameters (Least Square Method, 2010).

Table 6-5 Least Square Method Parameters

No.	ΔT (°C)	ΔV (V)	$x_i - \bar{x}$	$y_i - \bar{y}$			
i	x_i	y_i	x_i*	y_i*	x*y*	x*x*	y*y*
1							

$$\bar{x} = \frac{\sum_{i=1}^{n} x_i}{n} \quad \text{[EQ 6-1]}$$

$$\bar{y} = \frac{\sum_{i=1}^{n} y_i}{n} \quad \text{[EQ 6-2]}$$

$$b = \frac{\sum_{i=1}^{n} (x_i - \bar{x})(y_i - \bar{y})}{\sum_{i=1}^{n} (x_i - \bar{x})^2} \quad \text{[EQ 6-3]}$$

$$a = \bar{y} - b\bar{x} \quad \text{[EQ 6-3]}$$

Table 6-5 and EQs 6-1 to 6-4 present the procedure for calculation of best linear fit and correlation between dT and dV.

Least Square Method Result for NaCl Solution

Table 6-6 Least Square Calculation for the NaCl Solution

No.	ΔT (°C)	ΔV (V)	$x_i - \bar{x}$	$y_i - \bar{y}$			
i	$\bar{x}_1$	$\bar{y}_1$	x_i*	y_i*	x*y*	x*x*	y*y*
Σ	12.0408	-8.066	-30.9424E-11	-5.65276E-10	20929.02	158883.2	4395.631

Table 6-2 shows the calculation parameters for the least square results of CNT.

Thus,

a=-9.65183

b=-0.131726

For the correlation (Correlation, 2010):

$$\cos\theta = \frac{x^* y^*}{\|x\|\|y\|} = \frac{-20929.02}{\sqrt{158883.2}\sqrt{4395.631}} = -0.791953$$

This shows that the correlation/dependence between ΔT and ΔV for NaCl is 79.2%. As mentioned in Chapter 5, the voltage difference of NaCl solution is mainly due to the effect of thermophoresis, which also presents the thermoelectric property in the form of Seebeck coefficient.

Least Squares Method Results for CNT

Table 6-7 Least Square Calculation for CNT

No.	ΔT (°C)	ΔV (V)	$x_i - \bar{x}$	$y_i - \bar{y}$			
i	$\bar{x}_1$	$\bar{y}_1$	x_i*	y_i*	x*y*	x*x*	y*y*
Σ	7.441	-38.492	-5.7678E-11	-4.4711E-10	-292280	690023.5	855472.6

Table 6-2 shows the calculation parameters for the least squares results of CNT.

Thus,

a=-35.3407

b=-0.4235

For the correlation (Correlation, 2010):

$$\cos\theta = \frac{x^* y^*}{\|x\|\|y\|} = \frac{-292280}{\sqrt{690023.5}\sqrt{855472.6}} = -0.38042$$

This shows that the correlation/dependence between ΔT and ΔV for the CNT suspension is -0.38042. According to the character of carbon nano tubes (CNT), which has strong electric conductivity and thermal conductivity, the correlation between temperature and voltage gradient is not anticipated to be very strong (38%).

Least Squares Method Results for Al_2O_3

Table 6-8 Least Square Calculation for Al_2O_3

No.	ΔT (°C)	ΔV (V)	$x_i - \bar{x}$	$y_i - \bar{y}$			
i	$\bar{x}_i$	$\bar{y}_i$	x_i*	y_i*	x*y*	x*x*	y*y*
Σ	13.24814	-126.886	-6.92E-11	-2.13E-10	-11439.4	212314.8	85164.85

Table 6-3 shows the calculation parameters for the least squares results of Al_2O_3.

Thus,

a=-131.384

b=0.3396

For the correlation:

$$\cos\theta = \frac{x^* y^*}{\|x\|\|y\|} = \frac{-11439.4}{\sqrt{212314.8}\sqrt{85164.85}} = -0.08507$$

This shows that the correlation/dependence between ΔT and ΔV for Al_2O_3 suspension is -0.08507, which indicates that the correlation of temperature and voltage gradient is 8.5%. For bulk Al_2O_3 is not a typical thermoelectric material, it is not surprised that the correlation between ΔT and ΔV for Al_2O_3 suspension is low.

Least Squares Method Results for Bi_2Te_3

Table 6-9 Least Square Calculation for Bi_2Te_3

No.	ΔT (°C)	ΔV (V)	$x_i - \bar{x}$	$y_i - \bar{y}$			
i	$\bar{x}_1$	$\bar{y}_1$	x_i*	y_i*	x*y*	x*x*	y*y*
Σ	9.494	-144.982	-1.676E-11	-3.8E-10	-91489.9	82767.9	108205.7

Table 6-3 shows the calculation parameters for the least squares results for Al_2O_3.

Thus,

a=-134.487

b=-1.10538

For the correlation:

$$\cos\theta = \frac{x^* y^*}{\|x\|\|y\|} = \frac{-91489.9}{\sqrt{82767.9}\sqrt{108205.7}} = -0.96676$$

This shows that the correlation/dependence between ΔT and ΔV is 0.96676. As a suspension of a typical thermoelectric material, the strong correlation between ΔT and ΔV for bismuth telluride powder is very reasonable.

Table 6-10 Least Square Results for All Materials Tested

Material	Correlation	Thermoelectric	Explanation
NaCl Solution	79.2%	No	Thermophoresis
CNT Suspension	38.0%	Some	Conductor
Al_2O_3 Suspension	8.5%	No	Insulator
Bi_2Te_3 Suspension	96.7%	Yes	Thermoelectric Material

As a conclusion, Table 6-10 shows the least square results for all materials tested in these experiments. The thermophoresis effect presents the NaCl solution with a 79.2% correlation; 38.0% correlation for dT and dV was shown for the CNT suspension, while the bulk CNT is commonly regarded as conductor; for the Al_2O_3 suspension, only 8.5% correlation was shown, which is due to the characteristic of the bulk Al_2O_3, which is usually regarded as an insulator; as a bulk material with strong thermoelectric characteristic, Bi_2Te_3 suspension shows a very strong correlation (96.7%) for dT and dV.

f. Seebeck Coefficient Result for Bi_2Te_3

According to the results from the least squares method, the correlation of dT and dV for CNT and Al_2O_3 are low and thus should not be regarded as typical thermoelectric fluid suspensions. On the other hand, the Bi_2Te_3 nanoparticle suspension shows very strong thermoelectric characteristic, which is worth comparing with the bulk Bi_2Te_3 material. As Figure 6-10 shows, there is a best fit for the dV vs. dT curve for Bi_2Te_3:

$$\mathrm{dV} = -1.1054 * \mathrm{dT} - 134.49$$

Compare this equation to a standard thermoelectric equation:

$$\mathrm{dV} = \mathrm{S} * \mathrm{dT}$$

Therefore, the Seebeck coefficient for this linear fit is -1.1054mV/K.

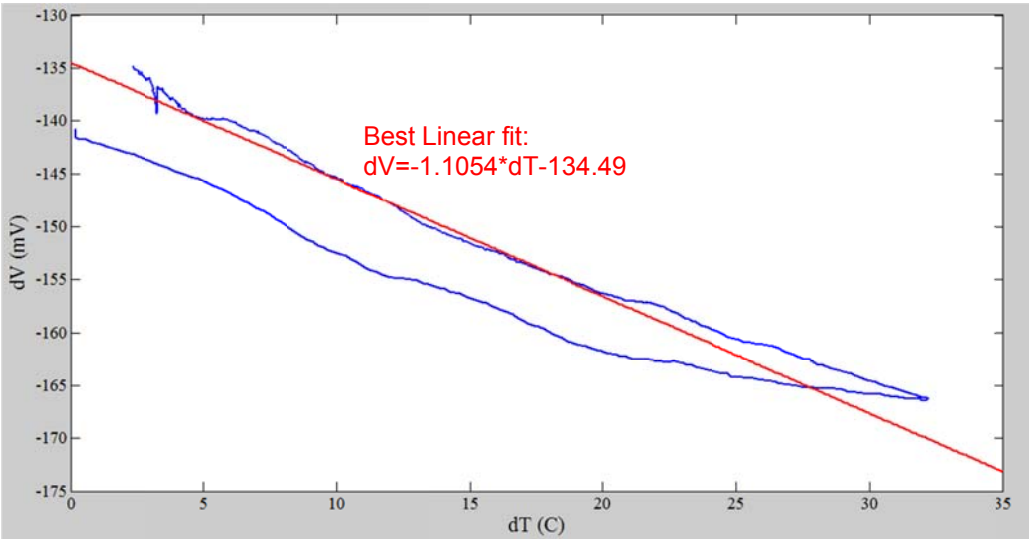

Figure 6-10 Seebeck Coefficient for Bi_2Te_3 Suspension

Nevertheless, as mentioned in the introduction, this Seebeck coefficient is not the Seebeck coefficient of the suspension, but the overall Seebeck coefficient of the suspension and probe wire that is used to

measure the voltage difference. The probe material is from the negative side of a T-type thermocouple, a copper-nickel alloy named constantan, with a Seebeck coefficient of -35μV/K (eFunda: Theory of Thermocouples, 2010).

$$S = S_{Bi} - S_{con}$$

Then the experimental Seebeck coefficient for the Bi_2Te_3 suspension would be:

$$S_{Bi,ex} = S + S_{con} = -1.1404\text{mV/K}$$

According to Chapter 1, the Seebeck coefficient of bulk Bi_2Te_3 is -287μV/K. Assuming that the Seebeck coefficient of the suspension is proportional to the volume fraction of nanoparticles, the anticipated Seebeck coefficient of the Bi_2Te_3 suspension would be:

$$S_{Bi,theo} = S_{Bi} * \text{Vol\%} = -287\mu\text{V/K} * 1\% = -2.87\mu\text{V/K}$$

It is obvious that the theoretical Seebeck coefficient is much smaller than the experimental value (only 0.24% of the experimental Seebeck coefficient), which indicates that the assumption for nanoparticle Seebeck coefficient does not apply.

Although it is pointed out that the thermophoresis effect in the fluid would affect the thermoelectric effect that's shown (Chapter 5), but the influence is not as big as it is shown in the experiment. Further research is needed for the explanation of this phenomenon and might be an effect that is worth exploring.

g. Experimental result for Bi_2Te_3 suspension without NaCl

As mentioned in the previous chapters, the NaCl was added to suspensions in order to eliminate the noises observed in the experiment. However, due to outstanding difference between the experimental Seebeck coefficient of Bi_2Te_3 suspension and anticipated Seebeck coefficient, another experiment on a Bi_2Te_3 suspension without NaCl added was performed.

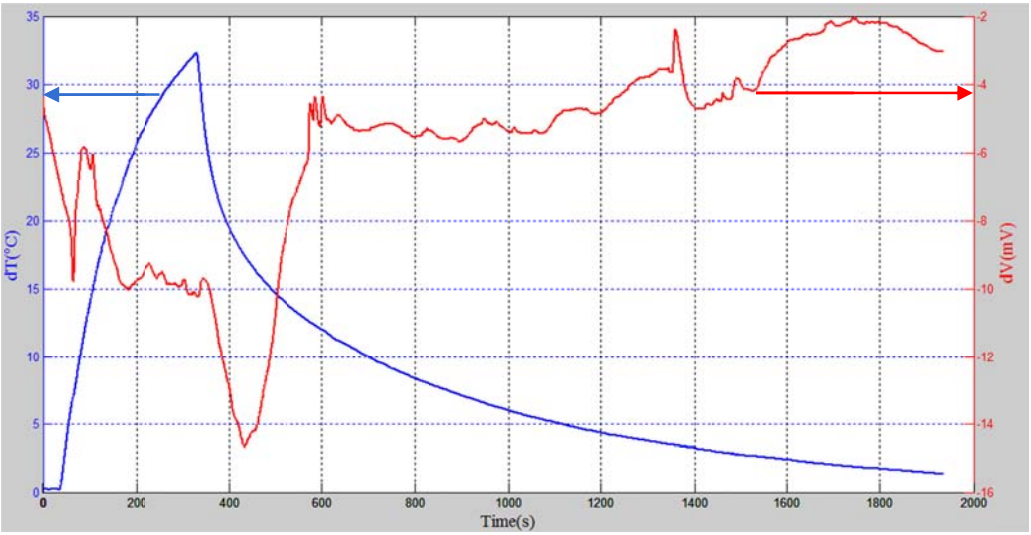

Figure 6-11 dT and dV for Bi_2Te_3 Suspension (No NaCl)

According to Fig. 6-10, the turning points of the two curves were not achieved at the same time. And the dV curve exhibited some noise as the experiment went on, which was also observed in other suspension experiments. The addition of NaCl greatly eliminated the noise measured in the experiments but at the same time changed the Seebeck coefficient of the suspension as well.

For the Bi_2Te_3 suspension without NaCl, the best linear fit is:

$$\mathrm{dV} = -0.29038 * \mathrm{dT} - 3.1358$$

Compare this equation to the standard thermoelectric equation:

$$\mathrm{dV} = \mathrm{S} * \mathrm{dT}$$

Therefore, the Seebeck coefficient for this linear fit is -290.38μV/K.

As shown in the previous section, the Seebeck coefficient of Bi_2Te_3 suspension with NaCl is -1.1404mV/K and the Seebeck coefficient of Bi_2Te_3 suspension without NaCl is -290.38μV/K, which is very close to the bulk material's Seebeck coefficient -287μV/K (Tan, et al., 2005).

It is clear that the NaCl in the suspension somehow magnified the Seebeck coefficient to -1.1404mV/k, with the rest of the parameters controlled to be the same. In the next chapter, a possible explanation for this phenomenon is discussed.

CHAPTER 7 Discussion of Seebeck Coefficient for Bi_2Te_3 Suspension

As shown in the previous chapter, the Bi_2Te_3 suspension with NaCl presents a very high Seebeck coefficient of -1.1404mV/K, while the Seebeck coefficient of the Bi_2Te_3 suspension without NaCl is -290.38μV/K. In this case, the NaCl solution not only eliminated the noise in the experiment, but also magnified the Seebeck coefficient of the suspension as well. In this chapter, the possibility of a magnified Seebeck coefficient is discussed in two parts: NaCl's thermophoresis effect and the thermoelectric characteristics of Bi_2Te_3 composites.

a. NaCl's thermophoresis effect

According to the analysis and discussion in Chapter 5, the maximum voltage difference due to the NaCl solution can be as large as -14.51mV. Assuming that part of the voltage difference is due to the thermophoresis effect of the NaCl solution in the Bi_2Te_3 suspension, the Seebeck coefficient shown by Bi_2Te_3 can be calculated.

The maximum voltage difference shown in the Bi_2Te_3 suspension with NaCl is -30mV. If the thermophoresis effect of NaCl solution is eliminated, the Seebeck coefficient of the Bi_2Te_3 suspension would be:

$$S_{Bi,sus} = \frac{dV_{Bi,exp} - dV_{NaCl}}{\mathrm{dT}}$$

$$= \frac{-30\mathrm{mV} + 14.51\mathrm{mV}}{32\mathrm{K}}$$

$$= -484\mu\mathrm{V/K}$$

According to the result, the estimated Seebeck coefficient for the Bi_2Te_3 suspension is -484μV/K, while the experimental result of the Seebeck coefficient for the Bi_2Te_3 suspension without NaCl is -290.38μV/K, which is 60% of the estimated Seebeck coefficient. The result of this assumption would not be sufficient to explain the high Seebeck coefficient observed in the experiment.

b. Thermoelectric characteristics of Bi_2Te_3 composites

It is shown in some research that Bi_2Te_3 composites show different thermoelectric characteristics compared to bulk Bi_2Te_3.

According to research on the thermoelectric properties of bismuth telluride-based alloys, the Seebeck coefficient of the $(Bi, Sb)_2(Te, Se)_3$ system varies with the percentage of C_{60} nanocomposites (N. Gothard G. W., 2009). It is also mentioned in the research that the C_{60} nanocomposites were added to decrease *ZT*, and the decrease of *ZT* in the experiment is that electrical conductivity decreases preferentially over lattice thermal conductivity (N. Gothard G. W., 2009). As indicated in previous research, the decrease of mobility leads to the decrease in electrical conductivity (N. Gothard J. S., 2010)

.A resent research shows that a peak *ZT* of 1.4 can be achieved in a p-type nanocrystalline $Bi_xSb_{2-x}Te_3$ bulk alloy at 100°C, while more significantly, this alloy maintains a *ZT* of 1.2 at room temperature and 0.8 at 250°C, which make it useful for both cooling and power generation (Bed

Poudel, 2008). The research also indicates that the p-type bismuth alloy reaches a peak of about 230μV/K at 100°C (Bed Poudel, 2008).

From the research mentioned in the previous paragraph, a high thermoelectric performance is shown in nanocrystalline $Bi_xSb_{2-x}Te_3$ bulk alloy. In this case, it is likely that a high thermoelectric performance can also be observed in nanoparticles or even in some nanoparticle suspensions (nanofluid), not only due to the thermophoresis effect of NaCl added to the suspension, but also due to the characteristic of the suspension itself. One of the reasons why the experimental Seebeck coefficient of the Bi_2Te_3 suspension without NaCl is similar to that of the bulk material is that the Bi_2Te_3 nanoparticles within the suspension were relatively stable; the nanoparticles were in good contact with each other, and the fluid increase the conductance between the particles; thus the Seebeck coefficient of Bi_2Te_3 suspension is close to the bulk material. On the other hand, the addition of NaCl solution might have changed the property of the nanoparticle suspension (in both thermoelectric characteristics and electric conductivity), and thus can lead to a suspension with even better thermoelectric performance.

CHAPTER 8 CONCLUSION

The introduction of this thesis presents a brief review of the history of thermoelectrics and the working principle of thermoelectric devices. Based on the thermoelectric effect shown in solid materials, an assumption is made that ‘nanoparticle liquid suspensions’ will share this characteristic as well.

One of the objectives of this thesis work is to develop an experimental procedure and setup proper experimental equipment to verify the assumption. In the experiment, three parameters are measured through the data logger: time, temperature and voltage. A verification test on the data logger is performed and double checked with the theoretical result of the copper wire, which would verify the performance of the data logger, excluding the possibility of a ‘ghost effect’ shown by the NI data acquisition block. Three different liquid suspensions (carbon nano tubes, aluminum dioxide nano powder and bismuth telluride nano powder) are tested in the experiment, and all are based on a 1% volume fraction NaCl solution.

The other objective of this thesis is to analyze the results of the experiment by comparing three different suspensions’ Seebeck coefficient and correlation between dT and dV. Due to the unique characteristics of three different nano particles (insulator, conductor and semiconductor), the correlation varies from 8% for Al_2O_3 to 38% for CNT and 96% for Bi_2Te_3. With discussion of the thermophoresis effect that existed in the NaCl

solution, a possible impact on voltage change across the temperature gradient is given in chapter 6.

The experimental Seebeck coefficient of the suspension for Bi_2Te_3 is -1.140mV/K, which is much more than expected. It would be of some interest if further research is focused on this phenomenon and might be able to develop a nanoparticle suspension with high thermoelectric performance.

There are a few works worth exploring in the future study of this thermoelectric effect in nanoparticle suspensions: a 2D/3D voltage gradient analysis in a 2D/3D temperature gradient; design an experiment with a closed loop to test the output power of the suspension in certain temperature gradient; further analysis on the relationship between thermophoresis and thermoelectric effect in the nanoparticle suspension; thermoelectric and heat transfer characteristics for nanoparticle suspension. With further research on the thermoelectric effect in nanoparticle suspensions, a flexible sensor using liquid or better thermoelectric fluid that dissipates the heat generated in electronic devices might be possible outcomes.

REFERENCES

Aluminum Oxide. (2010). Retrieved from MakeItFrom: http://www.makeitfrom.com/data/?material=Alumina

Correlation. (2010). Retrieved Nov 2010, from Wikipedia ZH: http://zh.wikipedia.org/zh/%E7%9B%B8%E5%85%B3

eFunda: Theory of Thermocouples. (2010). Retrieved Nov 2010, from eFunda: http://www.efunda.com/designstandards/sensors/thermocouples/thmcple_theory.cfm

Least Square Method. (2010). Retrieved from Wikipedia ZH: http://zh.wikipedia.org/zh/%E6%9C%80%E5%B0%8F%E4%BA%8C%E4%B9%98%E6%B3%95

A. Purkayastha, F. L.-T. (2006, Feb). Low-Temperature, Template-Free Synthesis of Single-Crystal Bismuth Telluride Nanorods. *Advanced Materials, 18*, 496-500.

A.I.Y. Tok, F. B. (2009). *Flame Synthesis of Nanoparticles*. Retrieved from Nanyang Technological University: http://www.mse.ntu.edu.sg/Research/Areas/Pages/FlameSynthesis.aspx

Bed Poudel, Q. H. (2008, May). High-Thermoelectric Performance of Nanostructured Bismuth Antimony Telluride Bulk Alloys. *Science*, 634-638.

DiSalvo, F. J. (1999, July 30). Thermoelectric Cooling and Power Generation. *Science, 285*, 703-706.

Huaqing Xie, H. L. (2003). Nanofluids containing multiwalled carbon nanotubes and their enhanced. *JOURNAL OF APPLIED PHYSICS, 94*, 4967.

Materialscientist. (2009, July 2). *File:Bi2Te3structure.jpg.* Retrieved from Wikipedia: http://en.wikipedia.org/wiki/File:Bi2Te3structure.jpg

Mills, B. (2008, June 15). *File:Corundum-3D-balls.png.* Retrieved June 1, 2010, from Wikipedia: http://en.wikipedia.org/wiki/File:Corundum-3D-balls.png

N. Gothard, G. W. (2009). Effect of Processing Route on the Microstructure and Thermoelectric Properties of Bismuth Telluride-Based Alloys. *CHEMISTRY AND MATERIALS SCIENCE, 39*, 1909-1913.

N. Gothard, J. S. (2010). *Physics Status Solidi A, 207*(1).

Newport. (2009). Retrieved from Newport Corperation: http://www.newport.com/

O. YAMASHITA, H. O. (2004). Effect of metal electrode on thermoelectric power in bismuth telluride compounds. *JOURNAL OF MATERIALS SCIENCE*, 5653.

Omega. (2010). *Thermocouple Reference Tables Type T.* Retrieved from OMEGA ENGINEERING, Inc.: http://www.omega.com/temperature/z/pdf/z207.pdf

Reilly, R. M. (2007). Carbon Nanotubes: Potential Benefits and Risks of Nanotechnology in Nuclear Medicine. *Journal of Nuclear Medicine, 48*, 1039-1042.

Sheng Zhang, J. L. (2004, June). Dissolution kinetics of galena in acid NaCl solutions at 25—75 °C. *Applied Geochemistry*, 835-841.

Tan, J., Kalantar-zadeh, K., Wlodarski, W., Bhargava, S., Akolekar, D., Holland, A., et al. (2005). Thermoelectric properties of bismuth telluride thin films deposited by radio frequency magnetron sputtering. *Proc. of SPIE, Vol. 5836*, 711-718.

Tellurex. (2010). *An Introduction to Thermoelectrics.* Retrieved 2010, from http://www.tellurex.com/technology/design-manual.php

Terry Hendricks, W. T. (2006). *Engineering Scoping Study of Thermoelectric Generator Systems for Industrial Waste Heat Recovery.*

Walter, K. (2007, May). *A Quantum contribution to Technology*. Retrieved from Science and Technology Review: https://www.llnl.gov/str/May07/Williamson.html

Wan, B. Y., Wang, W. L., Liao, K. J., & Lv, J. W. (2005). Seebeck Effect in Carbon Nanotube Films. *International Journal of Modern Physics, 19*, 643-645.

Würger, J. M. (2009). Thermophoresis at a charged surface: the role of hydrodynamic slip. *JOURNAL OF PHYSICS: CONDENSED MATTER, 21*.

APPENDIX A

MATLAB CODE FOR DATA DEMONSTRATION

(1)

```
clear all;
close all;
data=load('10_15_Bi2Te3_1%_NaCl_1%_Sur1%_run3(flipped).txt');
time=data(:,1);
time1=time(1:285);
time2=time(286:end);
dv=data(:,8);
dv1=dv(1:285);
dv2=dv(286:end);
dt=data(:,9);
dt1=dt(1:285);
dt2=dt(286:end);
s=data(:,10);
figure(1);plot(time1,dt1,'r');hold on;plot(time2,dt2,'b');
figure(2);plot(time1,dv1,'r');hold on;plot(time2,dv2,'b');
figure(3);plot(dt1,dv1,'r');hold on;plot(dt2,dv2,'b')
figure(4);plot(time,s);
```

(2)

```
clear all;
close all;
Bi=load('Bi_Seebeck.txt');
Al=load('Al_Seebeck.txt');
CNT=load('CNT_Seebeck.txt');
dT_Bi=Bi(:,1);
dT_Al=Al(:,1);
dT_CNT=CNT(:,1);
S_Bi=Bi(:,2);
S_Al=Al(:,2);
S_CNT=CNT(:,2);
plot(dT_Bi,S_Bi,'r');
hold on;
plot(dT_Al,S_Al,'b');
plot(dT_CNT,S_CNT,'g');
```

APPENDIX B

OTHER EXPERIMENT RESULT FIGURES

CNT Suspension Run 1

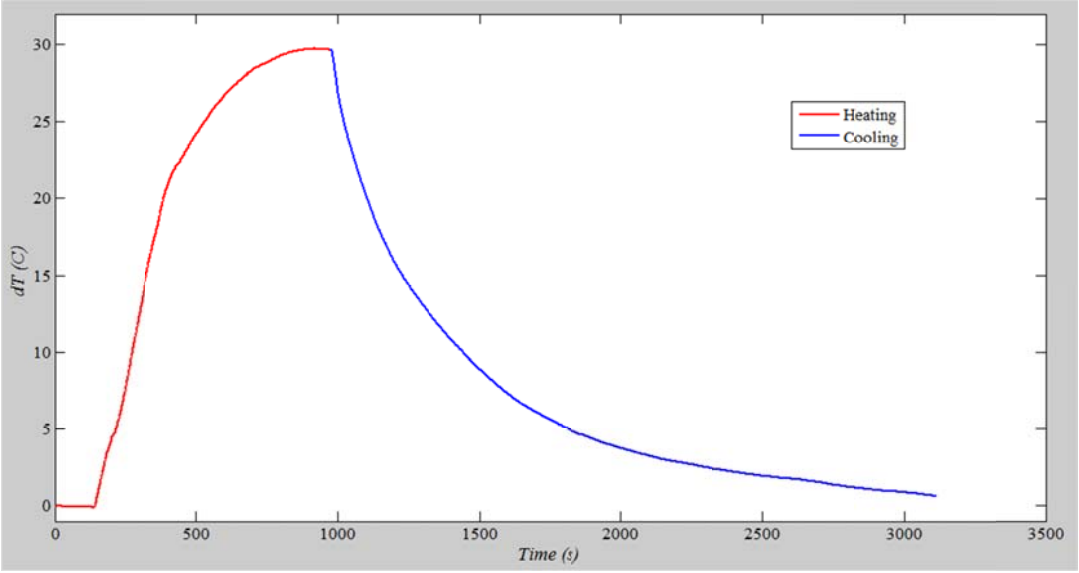

Time vs. dT

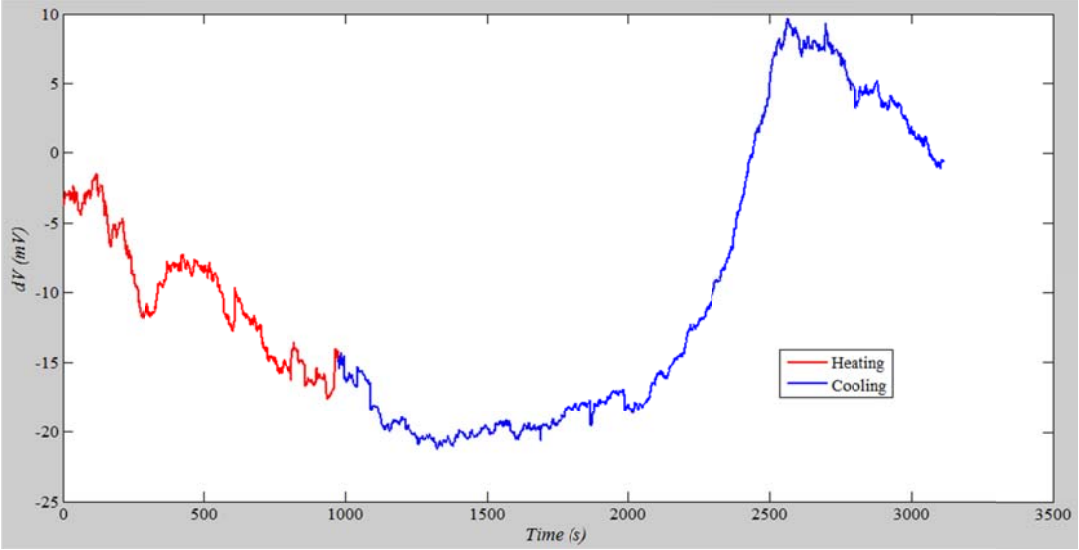

Time vs. dV

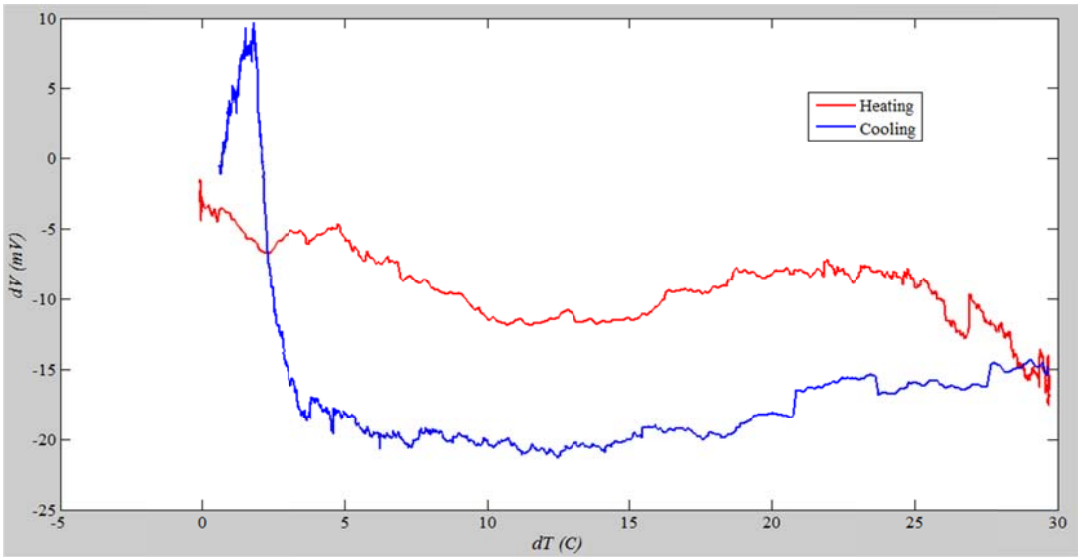

dT vs. dV

CNT Suspension Run 2

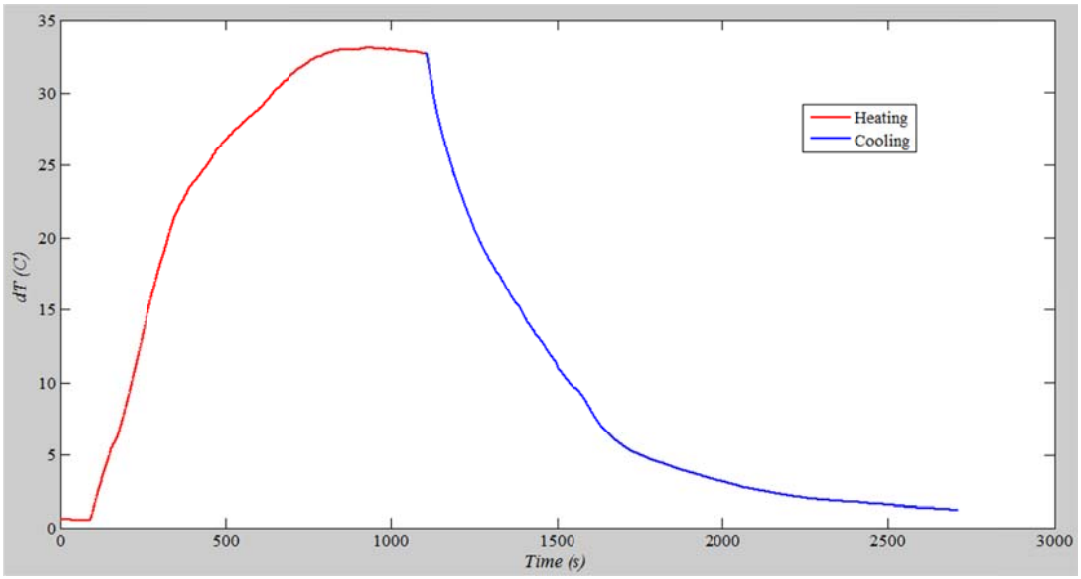

Time vs. dT

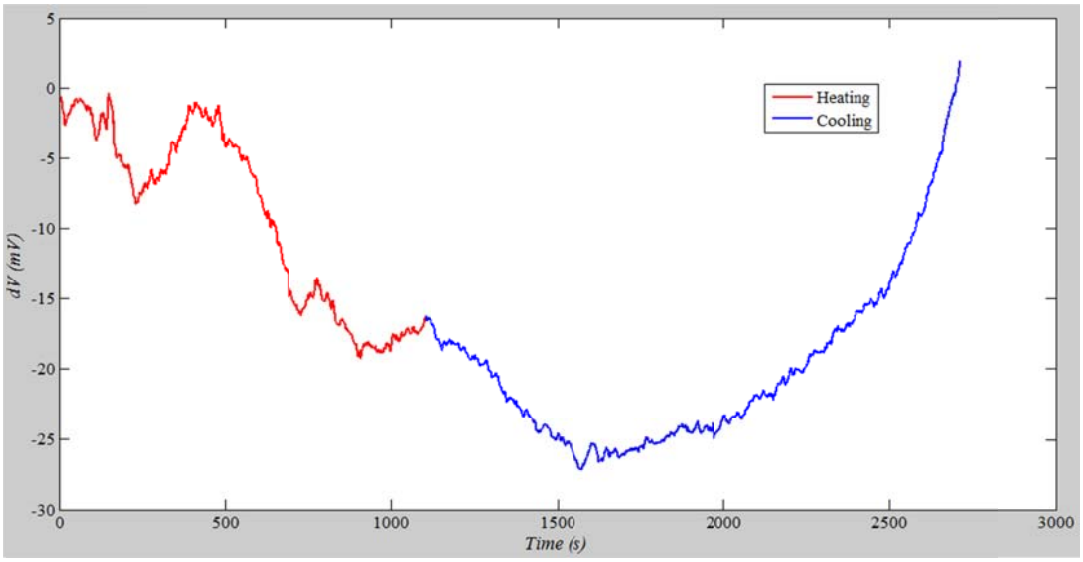

Time vs. dV

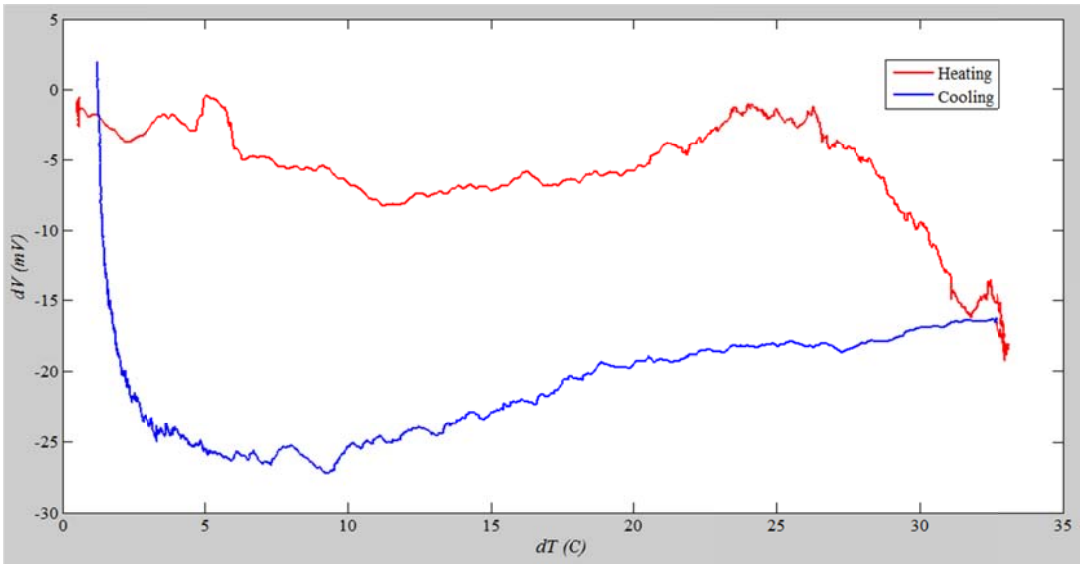

dT vs. dV

Al_2O_3 Suspension Run 2

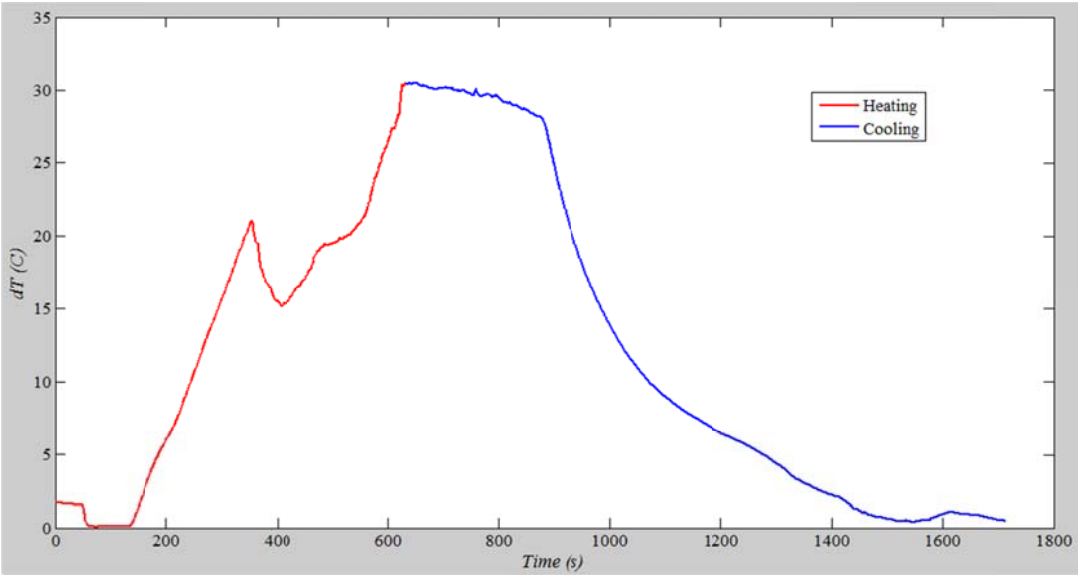

Time vs. dT

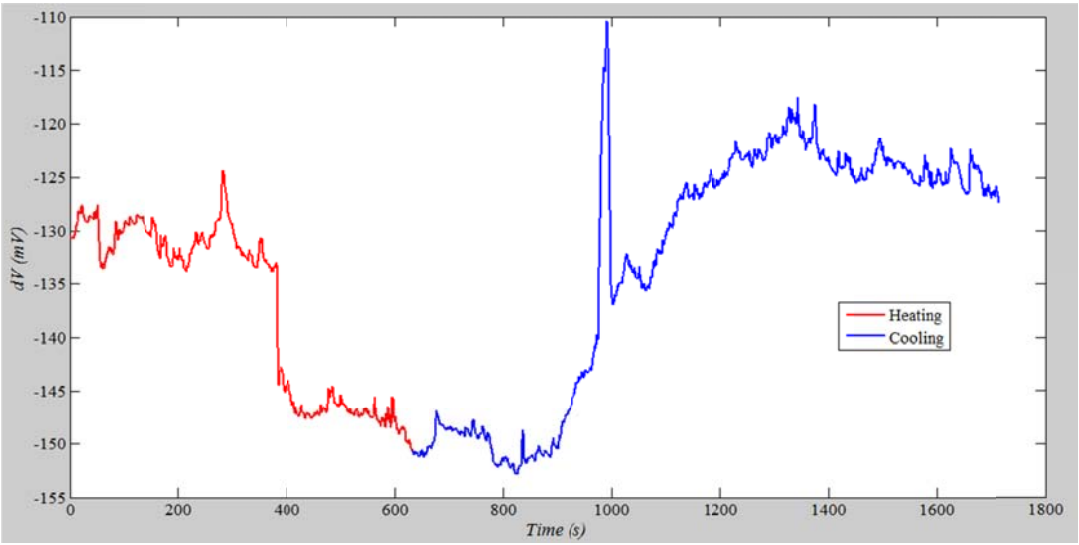

Time vs. dV

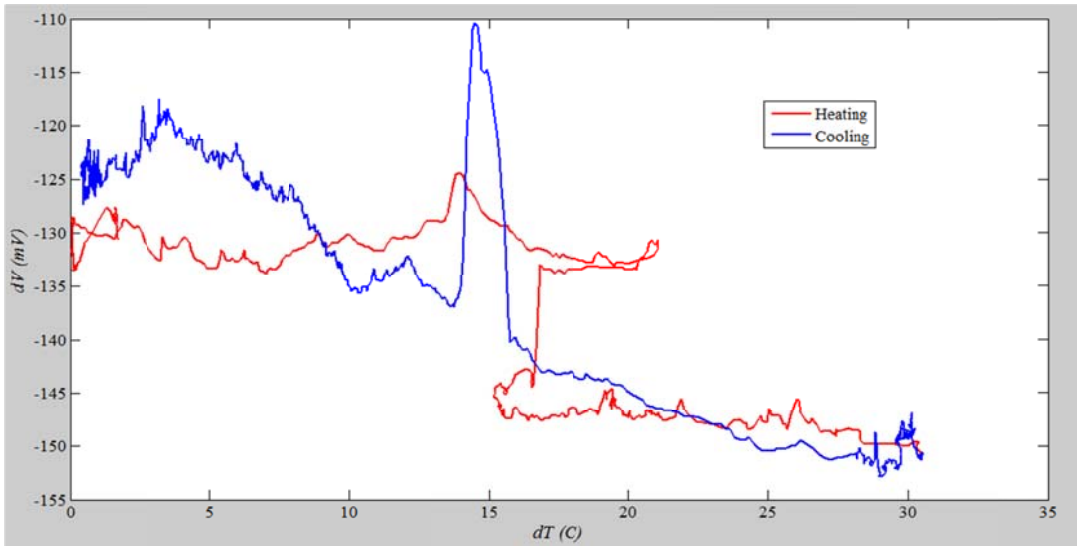

dT vs. dV

Bi_2Te_3 Suspension Run 1

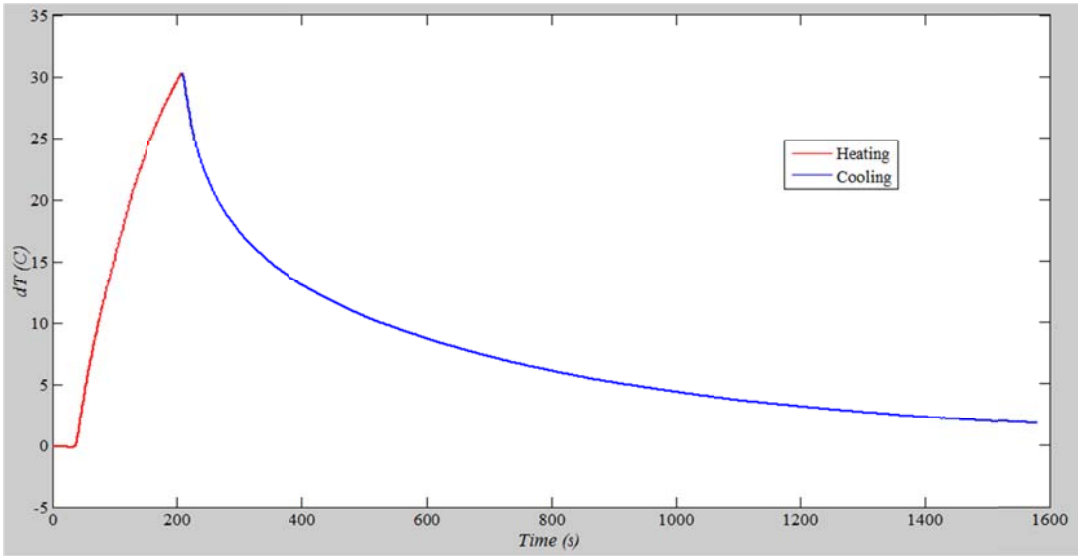

Time vs. dT

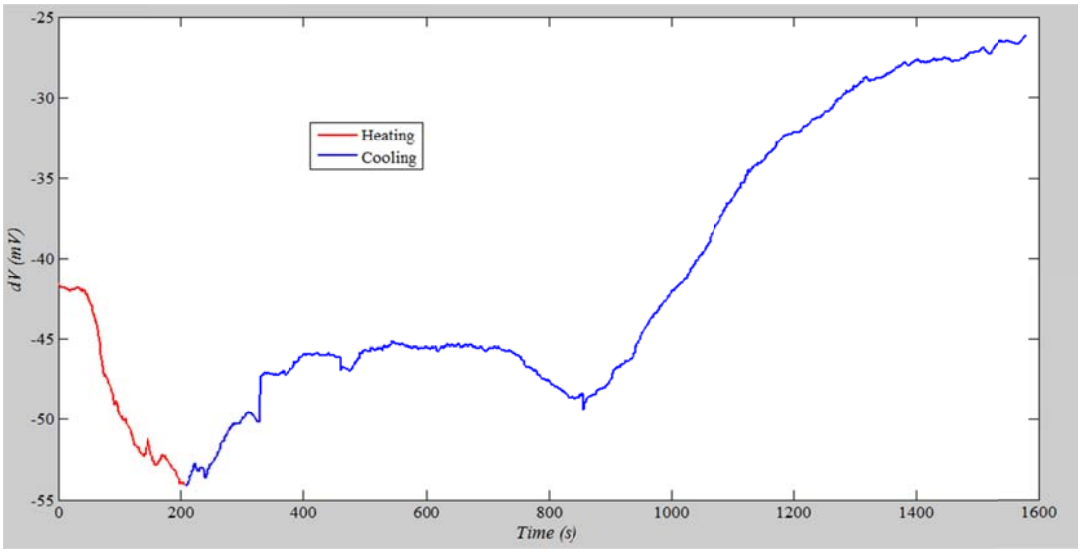

Time vs. dV

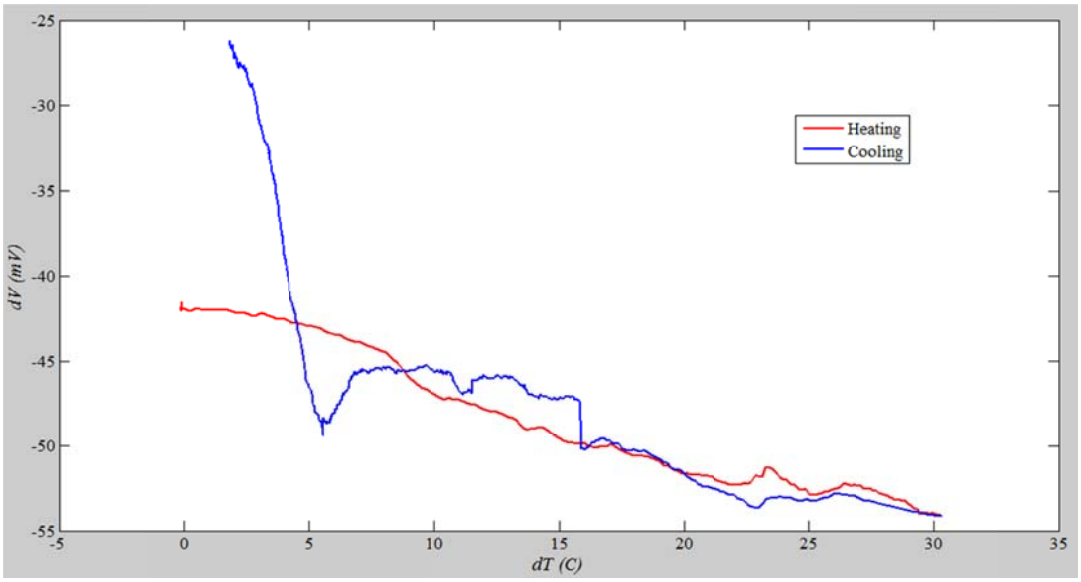

dT vs. dV

Bi_2Te_3 Suspension Run 3

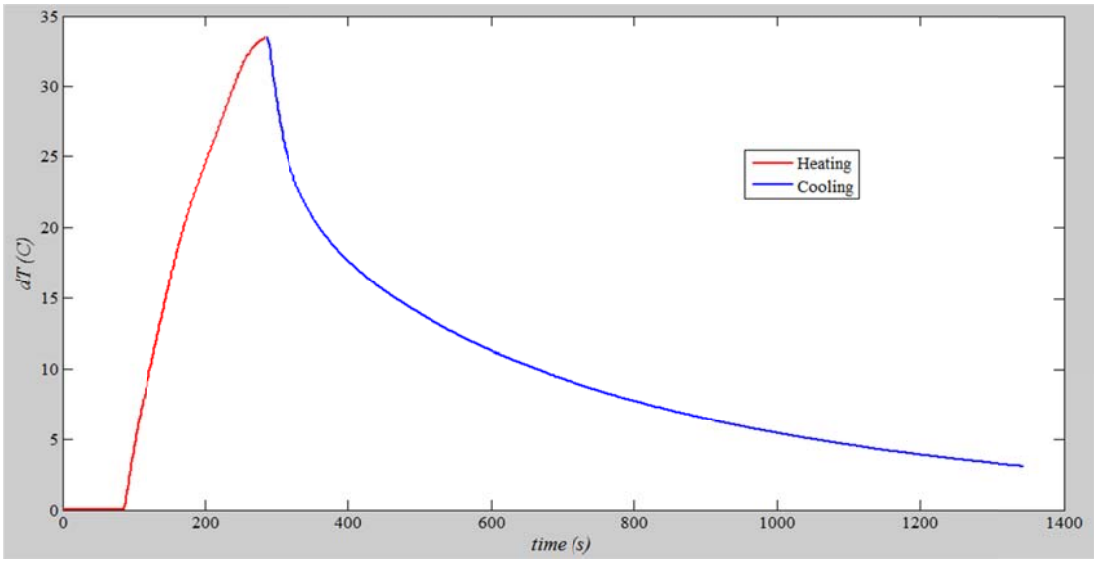

Time vs. dT

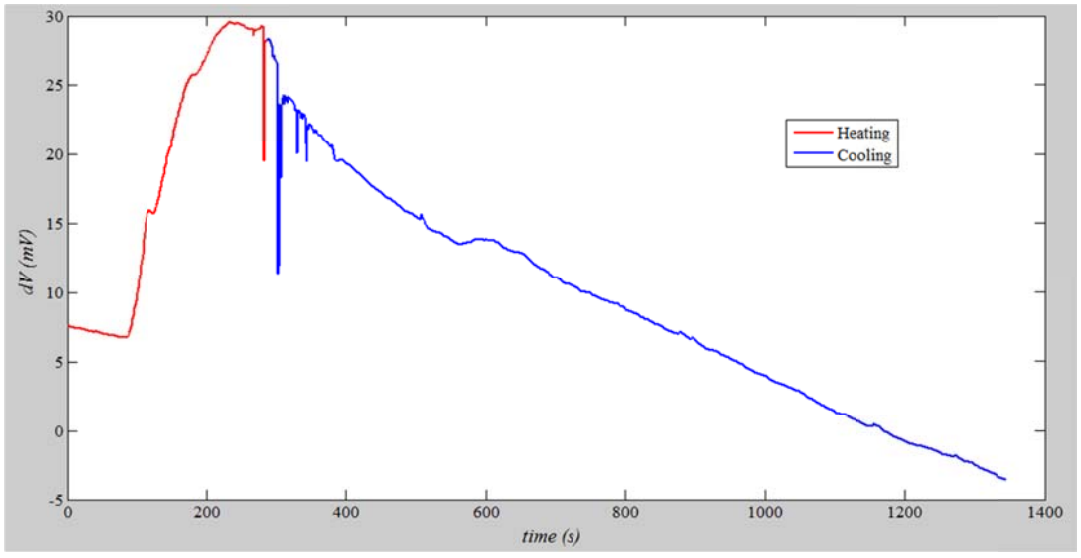

Time vs. dV

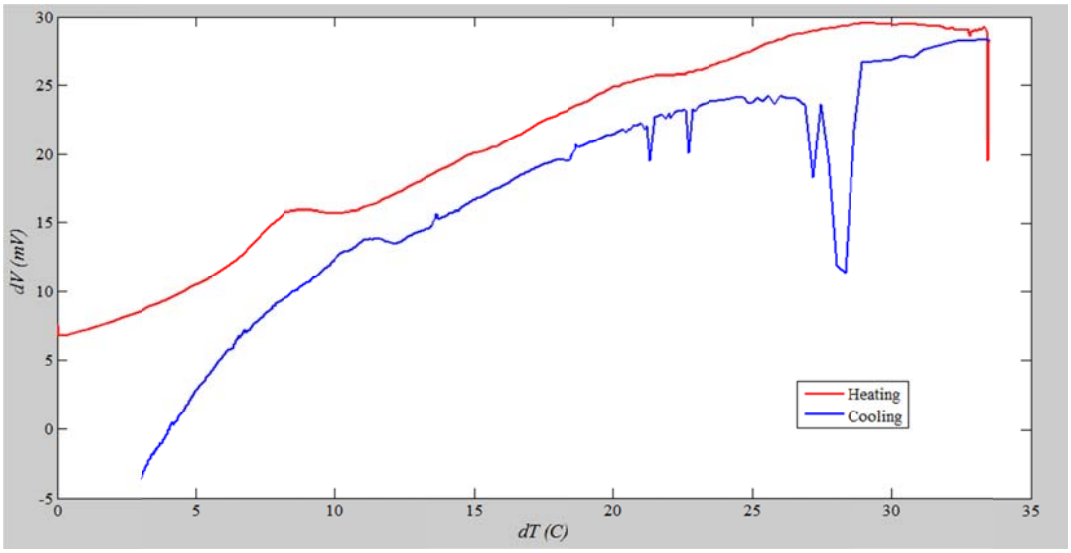

dT vs. dV